



TM-834  
1183.000

Fermilab Cancer Therapy Facility  
NEUTRON BEAM CALIBRATION AND TREATMENT PLANNING

M. Awschalom and Ivan Rosenberg

December 6, 1978

INTRODUCTION

The Cancer Therapy Facility at Fermilab (CTF); uses a fast neutron beam for research in cancerous tumor management.

This facility is one of only four now in operation in the USA. Hence, for therapeutic purposes, neutron beam calibration is a rare instance vis-a-vis photon beam calibration. Presently at each USA facility, the neutron beam has unique characteristics.

The description that follows has been prepared for medical physicists, radiobiologists, and radiotherapists considering or actually using the CTF for research.

For clarity, the presentation is divided into nine sections. They are:

- I. Brief description of beam line.
- II. Absolute in-phantom measurements. Interpretation of collected charge as muscle-tissue dose.
- III. Neutron beam flux monitors. Monitoring units.
- IV. Daily calibration of neutron beam monitoring units. Precision.
- V. Inter-institutional comparison of ionization chamber calibration using  $^{60}\text{Co}$ .
- VI. Dose distribution measurements. Techniques and instrumentation.
- VII. Beam characteristics. Parametrization.

VIII. Simulation and alignment systems. Checks and precision.

IX. Patient treatment planning.

In addition, there are fourteen appendices which include figures, tables and formulae. They are:

1. Beam line and collimator system.
2. Microcomputer calibration system: display of outputs.
3. Intercomparison results for  $^{60}\text{Co}$  calibrations.
4. Ionization chambers.
5. Collimators. Design, taper, materials, and activation.
6. Central Axis Depth Dose (CADD). Parametrization.
7. Tissue-Standard Ratios (TSR). Parametrization.
8. Off-Axis Ratios(OAR). Parametrization.
9. Wedge filter. Parametrization.
10. Alignment systems and checks.
11. Isodose distributions. Examples.
12. Radiotherapy documents.
13. Evolution of the treatment room.
14. Charge integrators.

I. BRIEF DESCRIPTION OF BEAM LINE

The 500-GeV proton accelerator at the Fermi National Accelerator Laboratory consists of four individual accelerators operating in series. The first three ("injector") operate at 15 Hz for 13/15 of one second to fill the vacuum chamber of the main accelerator with 8 GeV protons ("injection"). The acceleration of the protons to the chosen final energy(ies), extraction of the beam from the accelerator, and return of the magnetic field to injection conditions

takes from 8 to 15 sec. While acceleration is taking place in the main accelerator, the injector may be used for other purposes.

The neutron beam at the CTF is produced by the bombardment of a beryllium target with 66.18 MeV either protons or negative hydrogen ions. For this mode of operation the first accelerator, a Cockcroft-Walton (750 keV), and the first three sections of a nine section linear accelerator are used to impart energy to the protons or the negative hydrogen ions. This beam then drifts through linac tank four and it is extracted between sections four and five. It is then transported for a distance of about sixteen feet by a system consisting of two bending magnets (58 and 32 degrees respectively), seven quadrupole magnets, three beam position monitoring systems, and a noninterfering beam current monitor. See Fig. 1 in Appendix 1.

The beryllium target has a length of 22.1 mm and a diameter of 25.4 mm. This removes approximately 47 MeV from the protons. The residual energy is spent in a gold disk. Upstream from the target there is a tantalum collimator capable of stopping 70 MeV protons, and having a 5/8 inch hole in it. These components are mounted in a water-cooled aluminum holder. The target is electrically grounded. See Fig. 2, Appendix 1.

The target holder is surrounded radially and downstream by a steel block with an appropriately tapered hole to permit neutron fields of up to  $30 \times 30 \text{ cm}^2$  (42-cm diameter) at an SAD of 153.2 cm. This collimator is 12.5-cm long.

Following this primary collimator and attached to it are two transmission chambers. These chambers are described in Section III. Further on are the very thin aluminum mirrors for the field light and the coaxial laser beam.

Downstream from the mirrors there is a second section of the primary collimator that is 7.5-cm long. Then, the beam is shaped by polyethylene-cement collimators that are 93.6-cm long. This part of the collimating system is embedded in a concrete wall 101 cm thick. See Fig. 3 of Appendix 1.

## II. ABSOLUTE IN PHANTOM MEASUREMENTS. INTERPRETATION OF COLLECTED CHARGE AS MUSCLE-TISSUE DOSE.

It is assumed that a spherical, one cubic centimeter gas volume ionization chamber immersed in a large fluid mass does not violate significantly the requirements of the Bragg-Gray principles when used in the Fermilab p(66)Be(22 mm) neutron beam.

i. Ionization chamber wall. Absolute measurements are made with a spherical ionization chamber having walls, collectors, and guard electrodes made of Shonka's A-150 muscle-tissue equivalent plastic. These chambers are model IC-17. They were made by E.G. & G. The wall thickness is 5 mm.

ii. Medium. Most measurements are made inside a lucite phantom filled with a muscle-tissue equivalent solution. The solution has a density of  $1.07 \text{ g/cm}^3$ .

[See N. A. Frigerio et al, Phys. Med. Biol. 17, 792 (1972).]

- iii. Ionization chamber calibration. Annually, one of the ionization chambers is sent to NBS for calibration in their  $^{60}\text{Co}$  beam. NBS furnishes calibration certificated with a stated accuracy of  $\pm 2\%$ . No statement is made of the precision. We believe it is better than  $\pm 1/2\%$ . At NBS, the calibrations are made at 100 cm, at +600 volts, and at an exposure rate of approximately 1 R/sec.
- iv. Measurement of charge. All measurements are made using active integrators and analog-to-digital converters (ADC's and DVM's) having accuracies of  $\pm 0.1\%$  or better. The effective capacitance of the integrators is measured using precision air capacitors (General Radio, Type 1403) whose calibration is traceable to NBS with an uncertainty of  $\pm 0.01\%$ . ADC's and DVM's are calibrated using a semiconductor voltage source (COD1, Certacell) of 10.00004 volts  $\pm 5$  ppm.
- v. Measurement of time. Time is measured using a one megahertz crystal controlled oscillator. This frequency is known to  $\pm 0.01\%$ .
- vi. Measurement of temperature. Temperatures are measured continuously using copper-constantan thermocouples and digital read-outs. The calibration of the thermocouples and read-outs are checked using a mercury thermometer (Fisher Scientific Co., Model 15-041A) accurate to  $\pm 0.04^\circ\text{C}$  in the range  $10^\circ\text{C}$  to  $+50^\circ\text{C}$ . The thermocouple system is accurate to  $\pm 0.1^\circ\text{C}$  in the range  $20^\circ\text{C}$  to  $35^\circ\text{C}$  where it was tested.

vii. Measurement of pressure. A digital barometer (Datametrics Barocell #1174) is used to measure pressure continuously. Its accuracy is checked against a mercury barometer whose scale was adjusted at 740 mm to read 740.0  $\pm$ 0.5 mm at Fermilab.

viii. Charge collection efficiency. The ionization chambers are operated at +600 V (shell positive with respect to collector). In the  $^{137}\text{Cs}$  source, the collection efficiency is 99.96  $\pm$ .03%. In the neutron beam, the charge collection efficiency is about 99.9%. Hence no corrections are made for charge collection efficiency.

ix. Leakage current. Normally, the combined leakage current of the ionization chamber, interconnecting cable, and electrometer input current is not noticeably different from that of the cable and electrometer alone. This current is of the order of 5 fA. During dosimetry, the currents are about .2 nA, i.e. four to five orders of magnitude larger.

x. Interpretation of collected charge as dose. In agreement with the usage at American facilities, all ionization is assumed due to neutrons. Then, the neutron dose is given by

$$D_n = G_\gamma \times f \times A_{eq} \times \frac{W_{e,n}}{W_{e,\gamma}} \times \frac{S_{TE-air(n)}}{S_{TE-air(\gamma)}} \times K_{TE}^{muscle} \times \delta \\ \times (\text{Temp-Press-Corr}) \times Q$$

where

$G_\gamma$  =  $^{60}\text{Co}$  chamber sensitivity in R/C, given by  $^{137}\text{Cs}$  calibration

$f$  = R to rad conversion factor for muscle = 0.957 rad/R

$A_{eq}$  =  $^{60}\text{Co}$ -photon attenuation at the center of a minimum size "meat ball" (.5 cm radius)  
= 0.985

The values for the next five constants are those in use at TAMVEC (see A. Smith et al, Med. Phys. 2, 195 (1975)).

$$W_{e,n(\text{air})} = 35.8 \text{ eV/electron-ion pair}$$

$$W_{e,\gamma(\text{air})} = 33.73 \text{ eV/electron-ion pair}$$

$$S_{\text{TE-air}}(n) = 1.157 \text{ (stopping power ratio)}$$

$$S_{\text{TE-air}}(\gamma) = 1.142$$

$$\begin{aligned} K_{\text{TE}}^{\text{muscle}} &= \text{ratio of the kerma in A-150 to that in muscle-tissue} \\ &= (1.05)^{-1} \end{aligned}$$

$$\begin{aligned} \delta &= \text{displacement correction factor} \\ &[\text{see P. Shapiro, et al. Med. Phys. } \underline{3}, 87 \text{ (1976)}]. \\ &= 0.97 \end{aligned}$$

xi. Phantoms. For absolute dosimetry, measurements are made inside a parallelepiped made with 1/2 inch lucite sides except for entrance and exit windows that are 3 mm thick. The inside dimensions are (empty tank): parallel to beam direction, 36.9 cm; perpendicularly to the beam direction, vertically, 40.5 cm; horizontally, 44.0 cm.

For dose build-up measurements, an A-150 T.E. plastic cube was drilled perpendicularly to the center of one face. This provides a snug fit for an A-150 parallel plate extrapolation chamber made by EG & G, (Model EIC). This cube is approximately 20 cm to the side.

In addition to these two phantoms, there is a third one: an A-150 miniphantom used for daily calibration of the neutron beam. This miniphantom is a parallelepiped 15 x 15 x 16 cm.

The 16 cm dimension is parallel to the beam direction. It is mounted in a 1/2-inch thick lucite holder which covers five of its faces. It is marked to allow precise positioning of the center of the ionization chamber at the isocenter. A thermocouple is permanently inserted into the lucite. The center of the hole into which a 1 cc ionization chamber may be inserted is 9.73 cm from the entrance face. The beam entrance face is the only one not covered by lucite.

xii. Uncertainties. As described above, the major source of uncertainties in the accuracy of dose determination are:

- a - Chamber calibration by NBS ( $\pm 2\%$ ).
- b - Values for W, S, kerma ratio, and  $A_{eq}$ . The combined uncertainty of all these quantities should be about  $(10 \pm 5)\%$ .

The major sources of uncertainty in the precision of dose delivery are:

- c - ADC resolution and linearity ( $\pm 0.1\%$ ).
- d - Pressure (about  $\pm 0.1\%$ ).

### III. NEUTRON BEAM FLUX MONITORS. MONITORING UNITS.

i. Transmission ionization chambers. They are plane parallel structures made of aluminum and ceramic. They are enclosed in a common volume and use the same polarizing high voltage. The chambers are air filled and open to the atmosphere. The spacing between collector and polarizing plates is 2.9 mm. The chambers operate at a HV of +3000V. See Fig. 1 in Appendix 4.



ii. Beam on target monitor. A toroidal current transformer is placed upstream of the target to integrate the charge reaching the target.

iii. Reliability of operation. The outputs from the transmission ion chambers and the toroidal current transformer are integrated and digitized after each linac pulse (about 45  $\mu$ sec wide at 15 Hz). Then, the ratio of the output charges from the two transmission chambers and the ratio of the proton charge on target to the charge from the upstream transmission chamber are checked at one-second intervals. If these ratios fall outside narrow ranges, the operation of the CTF is inhibited.

iv. Temperature measurement. The temperature of the transmission ionization chambers is measured continuously with a copper-constantan thermocouple.

v. Utilization of the transmission chambers. The output of the transmission chambers is used to monitor the neutron fluence and terminate patient irradiations. This chamber system is calibrated to satisfy

$$D_n = K \times (\text{Temp-Press Corr}) \times \sum_i \Delta V_i \quad (\text{jig rad})$$

where

$D_n$  = is the neutron dose at the center of the ionization chamber in the miniphantom as measured with the 1 cc ionization.

K = calibration constant for the transmission chamber #1.

(Temp-Press Corr) = ideal gas correction factor

$\sum_i \Delta V_i$  = sum of the charge integrator output voltage at the end of "i" linac pulses (effectively the charge from transmission chamber #1).

This calibration is made using the 10 x 10 cm<sup>2</sup> collimator.

The dose delivered to this miniphantom may be related by appropriate TSR tables to dose to tissue at any depth for any collimator (see Sections VII. and IX.).

#### IV. DAILY CALIBRATION OF NEUTRON BEAM MONITORING UNITS. PRECISION.

The daily calibration of the neutron beam monitoring proceeds in three steps:

- i. ionization chamber calibration,
- ii. calibration of the neutron beam,
- iii. verification of proper microcomputer operation.

i. The ionization chamber (EG & G, Model IC-17 spherical, 1 cm<sup>3</sup>, TE) is calibrated in a <sup>137</sup>Cs irradiator using a highly reproducible geometry. The source strength has been calibrated in terms of effective <sup>60</sup>Co exposure rate for IC-17 chambers only immediately after an NBS calibration visit.

ii. The calibrated chamber is placed in the neutron beam, centered at the treatment isocenter inside the miniphantom. The neutron beam transmission chambers are calibrated such that one M.U. (monitoring unit) represents 1 Gy (1 Gray = 100 rad) in the miniphantom. The algorithm used is,

$$D_n \text{ (miniphantom)} = K \times (\text{T-P correction}) \times \sum_i \Delta V_i.$$

iii. A totally different manual system is used to verify that a dose requested from the computer is actually delivered to the miniphantom.

Steps i and ii are carried out automatically by the microcomputer. Facsimili of computer displays of calibrations are shown in Appendix 2.

iv. Precision in the calibration of the ionization chamber. The ionization chamber, as used in Fermilab, is only a transfer instrument to compare the exposure rate in a  $^{137}\text{Cs}$  calibrator to the neutron dose delivered to a special jig (miniphantom). A description of the stability of the calibration of a chamber is not useful since ionization chamber sensitivities are known to drift and even reverse their drift. A procedure in use at Fermilab to check the electronics may be used as a measure of precision of ionization chamber calibration.

In every patient treatment day the ionization chamber is calibrated in the  $^{137}\text{Cs}$ -source. Once a week, using a totally different set of electronics, the calibration is used to calculate the source strength. Since the two electronic systems are totally different, their drifts and noise must be independent of each other. The precision in the chamber calibration by one system must be better than the precision of source recalibration which involves two electronic systems. In the process of making the second

calculation, the ionization chamber is taken out from and reinserted into the  $^{137}\text{Cs}$  source. The strength of the  $^{137}\text{Cs}$  photon field source since March 29, 1978 (26 measurements) has been

$0.8716 \text{ R/sec} \pm 0.0010$  ( $\pm 0.12\%$ ), ( $^{60}\text{Co}$  equivalent) extrapolated to April 1, 1977.

v. Precision in the determination of K. Once the ionization chamber has been calibrated in the  $^{137}\text{Cs}$ -source, the conversion factor K of the transmission chamber is calculated daily. This calculation includes uncertainties in the ionization chamber calibration, positioning of the jig (miniphantom) at the isocenter, and electronic noise. The mean and standard deviation of the measurements for K, ever since the linac ion source was changed from  $\text{H}^+$  to  $\text{H}^-$  (six months) are

$9.153 \pm 0.048$  ( $\pm 0.52\%$ )  $10^{-3}$  neutron rad/volt.

V. INTER-INSTITUTIONAL COMPARISON OF  $^{60}\text{Co}$  IONIZATION CHAMBER CALIBRATION. To make valid intercomparisons of clinical

results in multi-institutional cooperative fast neutron beam therapy studies, it is necessary that there be agreement among the various medical institutions on delivered neutron doses to at least a phantom. Hence there have been a number of ionization chamber and beam dosimetry intercomparisons involving Fermilab, NRL, MD Anderson, U of Washington and GLANTA.

The results of the  $^{60}\text{Co}$  intercomparisons are given in Appendix 3.

## VI. DOSE DISTRIBUTION MEASUREMENTS. TECHNIQUES AND INSTRUMENTATION.

For all measurements except build-up, the ionization chamber is positioned in the T.E. liquid phantom by a three-dimensional scanner under microcomputer control. Various chambers are used to minimize displacement factor errors.

i. Positioning. The chamber is positioned by means of the four laser beams. It is placed at the isocenter after adjusting the phantom upstream side of the entrance window for the appropriate source-to-skin distance (SSD) and taking into consideration the bulging of the entrance window when the phantom is filled with TE solution.

The laser beams are also used to verify that the travel of the ionization chamber is parallel to the central axis of the beam. A maximum deviation of 1 mm over the full travel of the chamber is allowed. Then the phantom is filled with TE solution. The position of the chamber is changed and monitored remotely with the aid of a microcomputer.

ii. Output measurements. The dose per M.U. delivered at the center of the 1 cm<sup>3</sup> chamber in the standard miniphantom (jig) by the 10 x 10 collimator and that delivered per M.U. to the same chamber in the phantom were measured for a large number of collimators, both square and rectangular, at various SSD values and depths (z) in the phantom, always including the reference value of SSD = 143.2 cm and z = 10 cm for each. The jig would be measured both at start and end of each measurement session.

furthermore, a reference collimator, usually the 10 x 10 at SSD = 143.2, z = 10 cm, would be remeasured periodically to check for drifts. As many collimators as possible were measured in the same measuring session. Most collimators were measured at least on two separate occasions. The ratios of dose to the phantom per M.U. for each case (Gy/M.U.) to that of the standard miniphantom set-up (jig Gy/M.U.) are used to obtain "Tissue Standard Ratios" or TSR (Gy/jig Gy). These TSR's were parametrized and tabulated. See Section VII.

iii. Central axis depth dose. For the region extending from about 3 mg/cm<sup>2</sup> to about 7 g/cm<sup>2</sup>, a parallel plate extrapolation chamber (EG & G, Model EC) was used in a miniphantom. The charge collected at various depths is reported as dose even though the validity of this interpretation is questionable.

For the region extending from about 1.5 cm to 12 cm in TE solution plus window, a 0.1 cm<sup>3</sup> thimble chamber (EG & G, Model IC-18) was used.

For the region extending from 10 cm to 34 cm, the spherical 1 cm<sup>3</sup> chamber was used.

The 0.1 cm<sup>3</sup> and 1. cm<sup>3</sup> measurements are matched at 10 cm and 12 cm depth. The extrapolation chamber measurements are used from the minimum value to about 3 cm in depth, and are matched at 2 cm and 3 cm depth to the 0.1 cm<sup>3</sup> chamber readings. These measurements were made for at least one value of SSD for each collimator, and for some special ones at 3 or 5 different SSD

positions, sometimes repeating the same arrangement on two separate sessions. Enough information was thus collected to enable parametrization of the central axis depth dose data with varying collimators and SSD. See Section VII.

iv. Off-axis ratios. The measurements were made using the thimble  $0.1 \text{ cm}^3$  chamber at all times. For some collimators, data was collected at four to six different depths in the phantom, and at two or three different SSD positions, while all collimators were measured at least at one depth (and, if rectangular, in both dimensions). Enough information was thus collected to enable parametrization of the off-axis ratios with collimator width, depth and SSD. See Section VII.

## VII. BEAM CHARACTERISTICS. PARAMETRIZATION.

i. Collimator design. The taper of the collimator holes was designed to define field sizes at an SAD of 153.2 cm. The neutron source is assumed to be at the center of the Be-target. To illuminate the field with all of the possible neutron source, though the sides extrapolate back to a separation of 1.8 cm at the upstream face of the Be-target (1.1 cm from the center). See page 3. The geometry and dimensions of the tapers are given in Appendix 5, together with a list of available sizes.

The collimators are made of a mixture of polyethylene pellets, Portland cement and water. This concrete has a density of about  $1.6 \text{ g cm}^{-3}$ . The mixture is given in Appendix 5. A measurement of the long-time activation products produced by neutron spallation of this mixture is also given in Appendix 5.

ii. Central axis depth dose parametrization. The data obtained for a large number of collimators, both squares and elongated rectangles, at various SSD was analyzed by a multiparameter fitting program (MINUIT) available at Fermilab. The relative depth dose in the phantom was separated into geometrical and nuclear interaction factors. The inverse square law was assumed to hold from the center of the Be-target. The central axis depth dose (CADD) for any collimator could then be described as:

$$\text{CADD}(\text{coll}, \text{SSD}, z) = \left( \frac{153.2}{\text{SSD} + z} \right)^2 G(\text{coll}, \text{SSD}, z).$$

The function G was found to be dependent only on the side of the equivalent square at the surface of the phantom, when the side of the equivalent square is defined as [Ref: Sterling et al, Brit. J. of Rad. 37, 544, 1964]

$$\text{ESQ} = 2 \frac{S_W * S_H}{S_W + S_H} \text{ and}$$

where  $S_W$  and  $S_H$  are the projected sides of the field at the surface. (App. 5, Fig. 1) Thus, G becomes

$$G = G(\text{ESQ}, z).$$

This parametrization holds equally well for squares and elongate rectangles. The full algorithm is given in Appendix 6.

iii. Goodness of fit of the CADD algorithm. The parametrization described in Appendix 6 was applied to the 3 cm  $\leq \text{ESQ} \leq 30$  cm range. It reproduces all of the available data within the following tolerances: for 135.2 cm  $\leq \text{SSD} \leq 153.2$  cm;

$$6 \leq \text{ESQ} \leq 15; 1.5 \leq z \leq 24 \text{ cm; error } < 1\%;$$

$$3 \text{ cm} \leq \text{ESQ} \leq 6 \text{ cm and } 15 \leq \text{ESQ} \leq 30; z \leq 30 \text{ cm; error } \leq 2\%.$$

Some typical fits are shown in Appendix 6.



iv. Tissue standard ratios parametrization. The TSR is defined as the ratio of a dose in tissue (or phantom) at a given combination of field size, SSD, and depth to the dose at the fixed geometry of the miniphantom using the 10 x 10 collimator:

$$\text{TSR}(\text{coll}, \text{SSD}, z) = \frac{D_t(\text{coll}, \text{SSD}, z)/\text{M.U.}}{D_{\text{jig}}(10 \times 10, 143.5, 9.7)/\text{M.U.}}$$

where  $D_t$  and  $D_{\text{jig}}$  stand for tissue and jig doses respectively. Thus, the TSR can be thought of as tissue Gy/jig Gy. The measured values of TRS for SSD = 143.2, z = 10 for all available collimators were fitted by a least-square method as a function of "nominal equivalent square", that is the equivalent square at the isocenter (SAD = 153.2). This fit applies equally well to square and elongated rectangular fields, as is shown in Appendix 7.

To obtain TSR values at other SSD and depths, the following formalism was adopted:

$$\text{TSR}(\text{coll}, \text{SSD}, z) = \text{TSR}(\text{coll}, 143.2, 10) F(\text{SSD}) \left( \frac{153.2}{\text{SSD} + z} \right)^2 \frac{G(\text{coll}, \text{SSD}, z)}{G(\text{coll}, 143.2, 10)}$$

where function G was calculated from the CADD algorithm and  $[\text{TSR}(\text{coll}, 143, 10) * F(\text{SSD})]$  was the unknown. From the available measurements at various SSD for many collimators, the behavior of the function  $F(\text{SSD})$  could be analyzed and, incidentally, a check on the value of  $\text{TSR}(\text{coll}, 143.2, 10)$  obtained by fitting. The dependence of F on SSD was found to be very weak and similar

for all measured collimators. Therefore, a single algorithm was used for all collimators. See Appendix 7.

Finally, having achieved a satisfactory parametrization of the functions  $G(\text{coll}, \text{SSD}, z)$ ,  $F(\text{SSD})$  and  $\text{TSR}(\text{coll}, 143.2, 10)$ , the values of TSR at any SSD and depth can be tabulated using the above formula. See Appendix 7. These tables are used for patient treatment calculations.

v. Goodness of fit of TSR algorithm. As seen in Appendix 7, out of 15 collimators used for the original fit of  $\text{TSR}(\text{coll}, 143.2, 10)$ , no fitted value was more than 1% off from the measured one, and 7 were within 1/2% or less. All subsequent measurements on new collimators showed similar agreement with predicted values.

A total of 175 measurements on different collimators at various SSD and depths were compared to the TSR tables produced by the formulae in Appendix 7. Of these, 156 values were within 1% of predicted and all of them were within 2% of the tabulated values.

vi. Off-axis ratios parametrization. Three collimators were measured extensively for off-axis ratios, the 6x6, 10x10 and 15x15 cm<sup>2</sup>. Six depths were used at each of three SSD for these three fields. A smooth multiple function - multi-parameter algorithm was then fitted to all the data using the minimization of  $\chi^2$  method. The various free parameters of the algorithm were then analyzed for correlations with field size,

and depth (no significant correlation could be found with SSD, once geometrical magnification was taken into account). The final result is a single algorithm whose parameters are smooth functions of both field size and depth, which can be used to reproduce the off-axis ratio for any collimator at any SSD, any depth. The full algorithm is given in Appendix 8, together with some typical fits.

vii. Goodness of fit of off-axis ratios algorithm. The predictions of the algorithm of Appendix 8 were compared to measured OAR's for both square and rectangular fields. The only significant difference between, say, a 10x6 and a 10x15 profile was in the umbra region where the OAR is  $\leq 0.1$ .

There, the scattered dose well outside the beam edges, increases monotonically with the length of the orthogonal side. As the algorithm has larger uncertainties in that region, no attempt was made to correlate the parameters with the other dimension of the field, and the same OAR, for instance, is calculated for the two above examples. In summary, all measured OAR's are reproduced with the following uncertainties:

for 135 cm  $\leq$  SSD  $\leq$  153.2 cm; 3 cm  $\leq$  W  $\leq$  20 cm; 2 cm  $\leq$  z  $\leq$  30 cm;

(a) beam and penumbra, where OAR  $\geq 0.2$ , uncertainty  $\leq 2\%$ ;

(b) penumbra and umbra, where OAR  $\leq 0.2$ , uncertainty  $\leq 5\%$

viii. Wedge filters parametrization. Measurements of output, depth dose, and off-axis ratios were also performed for several collimators with a Teflon (PTFE) wedge filter of actual angle

of 31 degrees.

It was found that the attenuation factor of the wedge (WF) varied with collimator, having a linear correlation with the "nominal equivalent square". This dependence was parametrized as shown in Appendix 9. It is used in patient treatment calculations.

It was also found that the central axis depth dose with the wedge did not significantly differ from that without the wedge for all the collimators where it was measured, suggesting no appreciable alteration of the neutron energy spectrum by the wedge.

The influence of the wedge on the OAR was reproduced by an extra asymmetrical factor to the OAR algorithm, and its parameters were fitted as before, varying with field size and depth. See Appendix 9. The fitted and measured wedged OAR's were within the same uncertainties as the open field ones.

#### VIII. SIMULATION AND ALIGNMENT SYSTEMS. PRECISION.

i. System description. This system was conceptually designed by Lionel Cohen M.D., director of this facility. The patient positioning consists of several interacting components: two levels of coplanar laser beams, a field defining light, a moving platform, a patient immobilization device ("chair") on a movable and adjustable base, and a diagnostic X-ray machine with a calibrated lead marker graticule. A more detailed description is available in print (L. Cohen and M. Awschalom, Appl. Radiol. Nov-Dec 1976 p 51). The X-ray tube and the lasers at the higher level

reproduce the geometrical relationship of the neutron source and the lasers at the lower level, albeit with a  $180^\circ$  difference in orientation. See Fig.1, Appendix 10.

Patient positioning is achieved with the following steps:

(1) The patient is immobilized relative to the restraining device usually by means of a custom-made cast. The desired entrance points for the beam axis for the various portals (and the field sizes) are determined at the initial planning session by means of diagnostic (planning) radiographs, with the lead markers of the calibrated graticule defining the central axis and the actual dimensions at the isoplane (usually mid-plane of the target volume).

(2) Positioning and adjustments are made using two orthogonal translational motions and the rotational ability of the chair base as well as the vertical motion of the platform. The position of the base is, however, fixed relative to horizontal rails at the point which puts the vertical axis of rotation through the isocenter (X-I/C). See Appendix 10. This isocentric arrangement allows change from portal to portal, in most cases, by rotation only.

(3) Reference points are then drawn on the patient's skin or cast for each portal using the laser beams at the X-ray level (X-lasers, referred to as North, South, East and West according to the wall on which they are mounted) and the X-ray central axis.

(4) The patient is then (and at each treatment) lowered with the moving platform to the neutron level, rotated through

180° and translated to the neutron isocenter. Then the laser beams fall on the corresponding marks on the skin or cast. This dual level arrangement minimizes the time that the technologists need to spend near the neutron beam collimator. The occupational exposure from remnant radioactivity is thus kept well within safe limits.

(5) The field defining light is used to define and check the edges of the treated areas on the skin of the patient (these can also be drawn on the skin or cast as further reference points).

Using the marks on the cast, the cast reference parameters relative to the restraining device, and the chair base coordinates (x, y and rotation angle), as well as the drop of the platform, the patient can be quickly re-positioned at every treatment session at the X-I/C using the X-lasers as reference. The transfer of the patient to the treatment position is then simply achieved by a further fixed drop of the elevator and a translation of the base along the rails to the n-I/C coupled with a 180° rotation, with no further adjustments. The n-lasers (and the field marks) serve as a further check on the reproducibility of the position. The desired position can be confirmed in most cases by a neutron radiograph showing salient anatomical structures in relation to the beam edges, to be compared to the original planning films.

To achieve this accurate positioning in the shortest time for each patient every day, all components of the system must

be correctly aligned and consistent with all others. The requirements for this compatibility are best broken down for each component; this is done in Appendix 10.

ii. Checks and precision. Checks of the above requirements are performed at regular intervals, some on each patient treatment day, others weekly or monthly. Special precision frames have been designed to make most of these checks simpler and more reliable. The alignment of the X-ray focus to the laser beam and graticule is checked by taking a radiograph of a lead cross positioned concentrically to the laser beams. The coincidence of the neutron and light fields is checked by taking a neutrogram of an open field after marking the field light and beam laser on the film. Most checks reproduce the positioning relative to the lasers to within 1 mm, and no part of the system is allowed to drift out of alignment by more than 2 mm before action is taken to correct it.

## IX. PATIENT TREATMENT PLANNING.

i. Collimators. Owing to the fixed horizontal beam design of the facility, individual collimators are used to define the fields for patient treatment. Thus, one is restricted to a finite, if large, choice of fixed sizes. The list of available collimators is given in Appendix 5.

ii. Computerized treatment planning. The various algorithms for central axis depth dose, off-axis ratios and wedge filters

are integrated into a complete treatment planning system run on a Fermilab computer. This system includes facilities for entering the patient contours and internal structures, together with the location and orientations of the beams, with a magnetic tracing device, for modifying the plans and viewing the isodose distribution on a vector scope terminal, and for drawing them on an incremental plotter, as well as copying them straight from the terminal, with all relevant information. The calculations use information from the contour to allow for non-normal incidence; no corrections for inhomogeneities are made at present. Examples of isodose distributions obtained with this system are shown in Appendix 11.

iii. Mixed beam planning. As the bulk of the system was obtained with the kind help of Rush-Presbyterian St. Lukes physics department (and modified for neutron beam use), there are intrinsic capabilities to simulate  $^{60}\text{Co}$  (Theratron 80) and 4 MeV (Clinac 4) X-ray beams, as well as the Fermilab neutron beam, on the same plan; 6 MeV (Varian) X-rays and electron beams up to 35 MeV will be added in the near future. This capability is extremely useful, in view of the large number of cases that are treated on mixed-modality protocols. Examples of these capabilities are shown in Appendix 11.

iv. Central axis beam calculations. Once the final treatment plan has been approved by a radiation oncologist and the isodose level at which the Minimum Tumor Dose should be delivered



has been decided, the TSR Tables are used to calculate the Monitor Units required to deliver the correct daily dose to the target volume from each field.

The Monitor Units are calibrated so that 1 M.U. delivers 1.0 Gy to the ionization chamber in the miniphantom (see Section IV.) and thus can be called 1 jig Gy. Therefore to deliver a dose D(Gy) at a depth x, at a given SSD, using a chosen collimator and, if required, a wedge filter and other absorbers:

$$\text{M.U.} = \frac{D}{\text{TSR}(\text{coll}, \text{SSD}, z) * \text{WF} * F} \text{ jig Gy}$$

where TSR is in Gy/jig Gy, WF is the wedge absorption factor (<1), tabulated from the algorithm in Appendix 9, and F is any other factor that affects the dose delivery (e.g. tray factor).

v. Treatment Chart and Mixed Beam Forms. The special circumstances of the Cancer Therapy Facility require the design of specialized documents to record and transmit radiotherapy information. Most of the records of treatment in this facility will sooner or later have to be reviewed for statistical analysis. Thus, a treatment record chart was designed to clearly differentiate between physical neutron dose and equivalent dose in the prescription and to record other concomitant treatment options. It was laid out keeping in mind clarity of reproduction and interpretation by outsiders. See Appendix 12.

The CTF is in the unique position among neutron therapy facilities in not being linked to any one radiation therapy department. Therefore, its mixed-modality patients are treated

at two separate institutions, often by different radiation oncologists and physicists. Communications in such circumstances are not always easy, and must be planned carefully so that patient care does not suffer. To this end many specialized forms for mixed-modality treatments of various sites have been evolved to exactly describe both arms of treatment as concisely as possible. Some examples are shown in Appendix 12.

vi. Simulation and verification. The calibrated graticule in front of the X-ray simulator helps define both the center and the borders of the planned field. Verification radiographs and neutrograms are taken at regular intervals to assure that the planned treatment is carried out, and they are compared to the initial planning films and to the isodose plans.

### Acknowledgement

The Cancer Therapy Facility at the Fermi National Accelerator Laboratory was funded on June 29, 1975, and the first patient was treated on September 7, 1976. During these fifteen months a crude facility was built, in which dosimetry and radiobiology experiments were performed, then it was torn down, and a suitable facility rebuilt.

So much was possible in such a short time only because many people, too many to mention individually, helped unselfishly. Help was received from medical institution in Chicago and elsewhere and from Oak Ridge National Laboratory, Argonne National Laboratory, Los Alamos Scientific Laboratory, Illinois Benedictine College and the Naval Research Laboratory. It goes without saying that Fermilab did the lion's share of the work, particularly its Accelerator Division and the CTF staff.

To these many helpers we give our thanks.

# Comparison of Some Parameters of Accelerator Produced Neutron Beams

Institution Parameter	Fermilab	Hammersmith (1)	University Washington	NRL (2)	M.D. Anderson T.A&M U. (3)	Medical Cyclotron (4)
particle	p	d	d	d	d	p
target	Be	Be	Be	Be	Be	Be
incident energy (MeV)	66	16	21.5	35	50	42
beam power (kw)	.53	1.3	.86	.35	.35	3.
mean neutron energy (MeV)	25±2	7.6	8	15	21	~20
SAD (cm)	153	116	150	125	140	125.
depth of Dmax (g/cm <sup>2</sup> ) (5)	1.7	0.23	0.30	.55	1.07	—
depth of 50% Dmax (g/cm <sup>2</sup> ) (5)	14.9	8.8	10.2	12.8	13.8	14.7
beam current (mA)	.020 (6)	.080	.040	.010	.007	.047
tissue dose rate at Dmax at stated SAD (rad/min) (5)	45	43	~40	66	60	47.

(1) Hammersmith Hospital, MRC  
London, England.

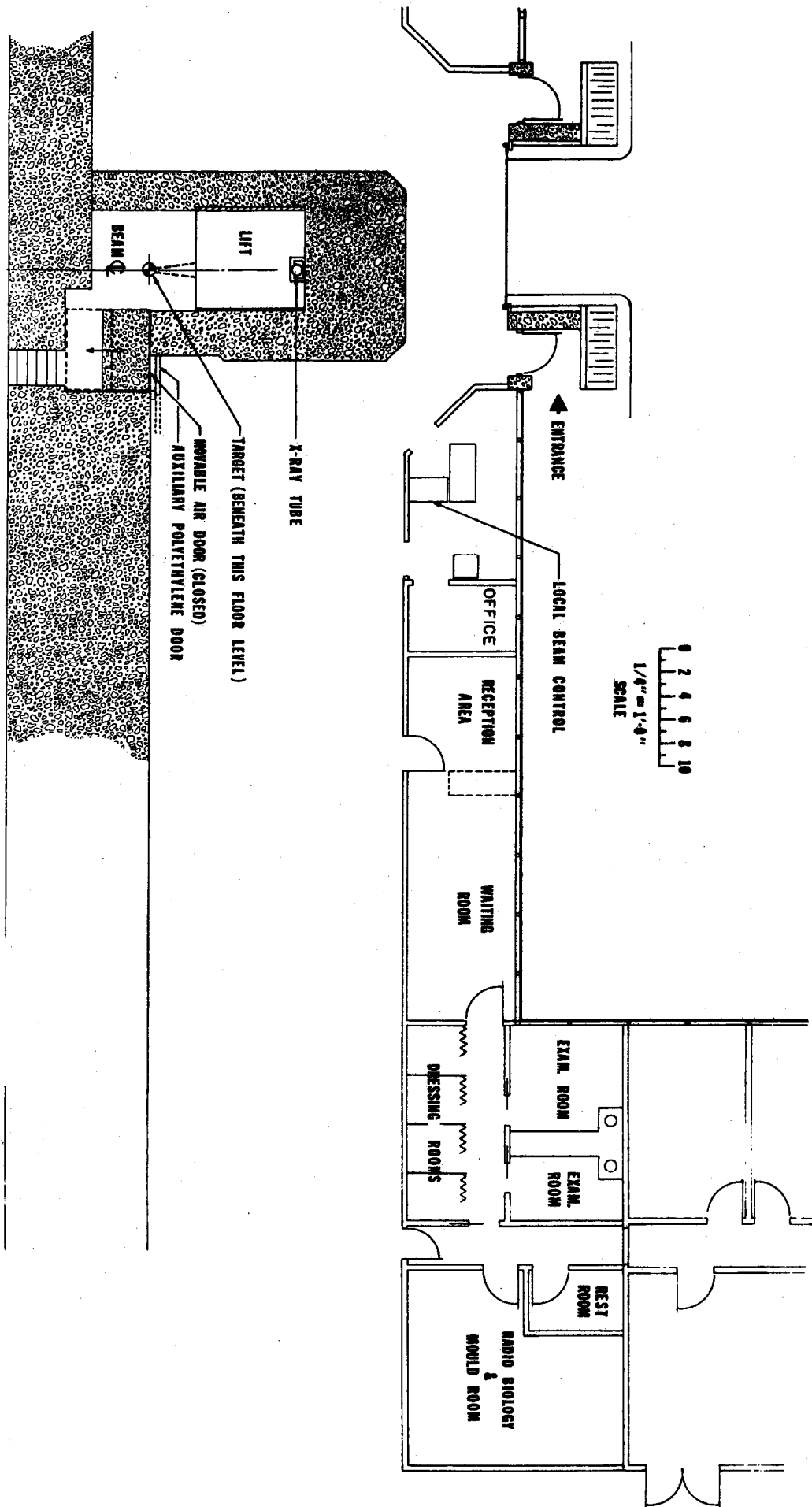
(2) Naval Research Laboratory  
Washington, D.C.

(3) M.D. Anderson Hospital & Texas A&M University  
Houston, Texas.

(4) Data taken from brochure published by the  
Cyclotron Corp.

(5) 10 cm x 10 cm field at stated SAD.

(6) Linac pulse modulation for High Energy  
Physics



## APPENDIX 1

### Beam Line. Collimator System.

Figure 1 shows the 66MeV proton beam line from the extraction point at the high energy end of tank #4, to the beryllium target as well as the location of the neutron beam collimators, shielding walls, and the moveable shielding block that allows access to the target area for maintenance.

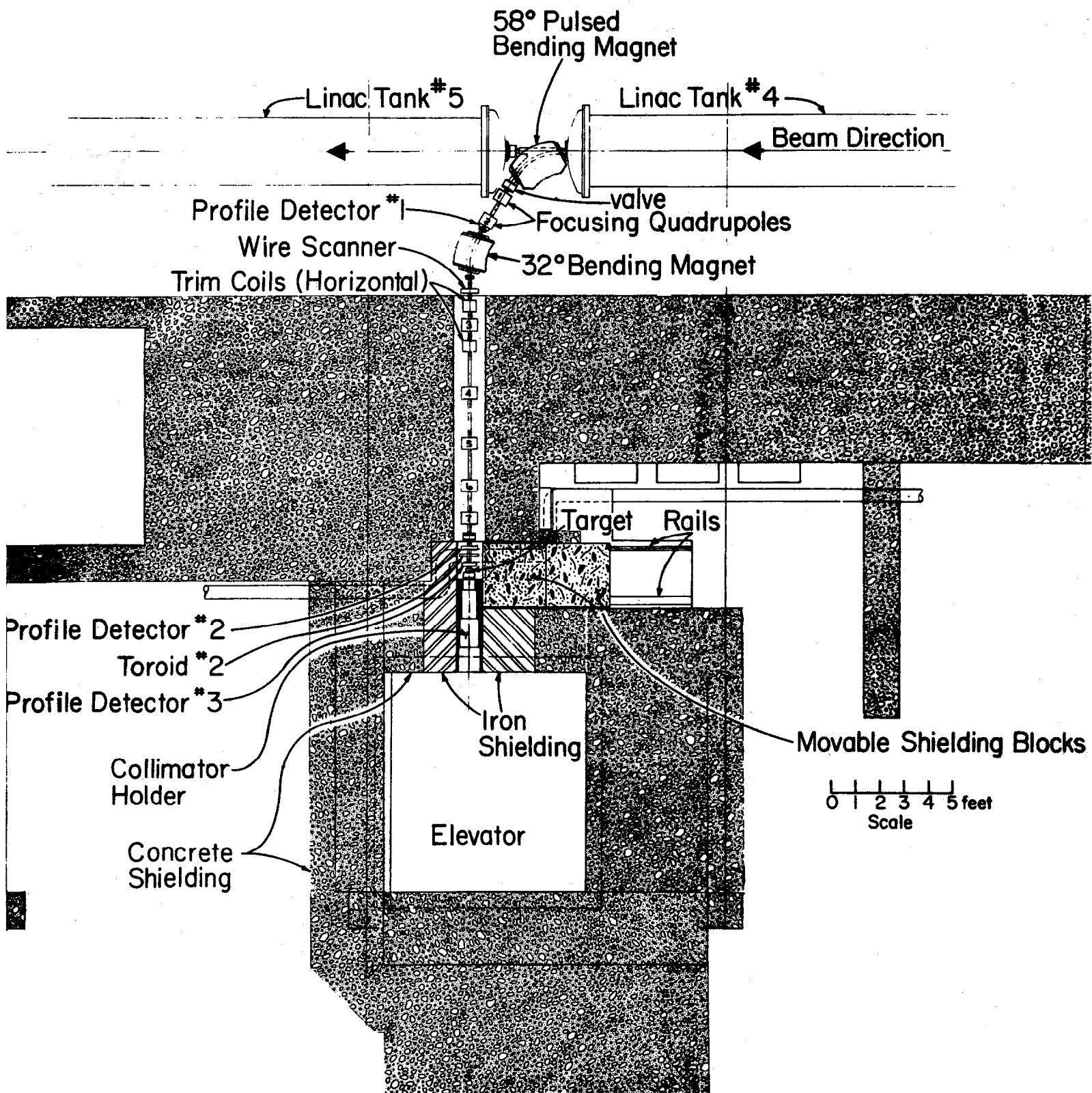
Once beam is requested and the safety system and control computer allows it, the 32° bending magnet is energized until the end of the requested neutron dose. The 58° bending magnet is turned on and off in such a manner that beam is allowed to go to the main accelerator as needed for high energy physics (HEP) research and to the Cancer Therapy Facility when not needed for HEP. It takes approximately 0.6 seconds for this magnet to transition from one state to the other.

Figure 2 shows the target assembly in detail. The various subcomponents are labelled in Figure 3.

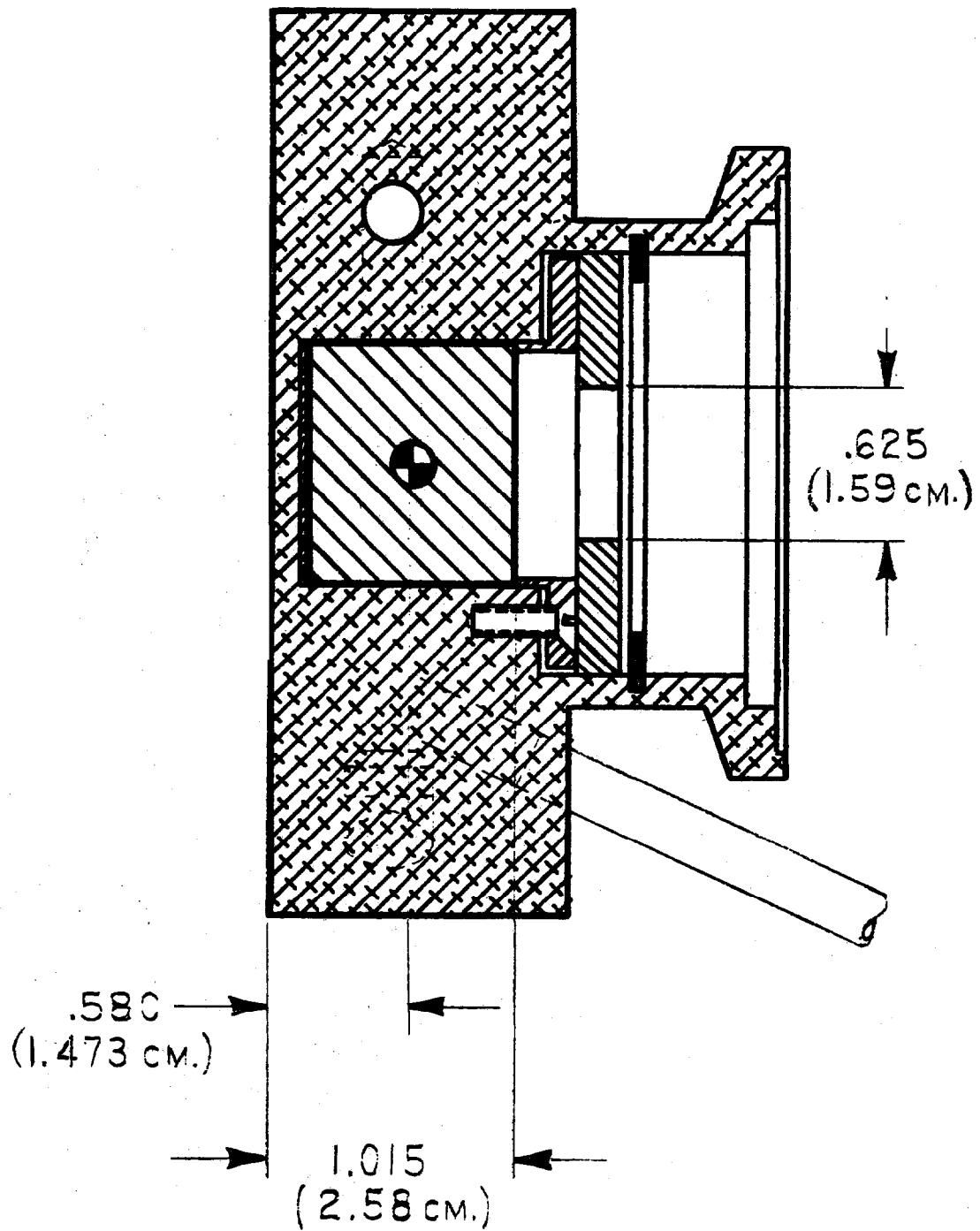
Figure 3 shows the target assembly inside the steel pre-collimator which holds the assembly of the dual transmission ionization chamber. Following this assembly are the adjustable mirrors for the co-axial laser beam and the field light, a second section of the primary collimator, and then the holder for the collimators. The shaded insert labelled "LINER" and the inner steel pieces from D4 to D4" may be removed to allow the insertion of larger collimators. Small collimators permit square fields of up to 15x15 cm<sup>2</sup>, large ones up to 30x30 cm<sup>2</sup>.

Figure 4 shows how the linac time is divided between high energy physics, transition times for the 58° bending magnet, and Cancer Therapy. The main ring cycle depicted is 10 seconds long; however, this time may vary from 7 to 16 seconds depending on energy, length of flat top (extraction time), and time of day (which affects cost of electrical power).

Figure 5 shows the functions of the beam line microcomputer that monitors beam line operations, safety, and beam delivery. This microcomputer is set-up for treatment by the medical microcomputer. The final command to begin treatment is effected depressing simultaneously two widely separated switches. The microcomputers are built around the MM6800 microprocessor.



APP. 1, Fig. 1

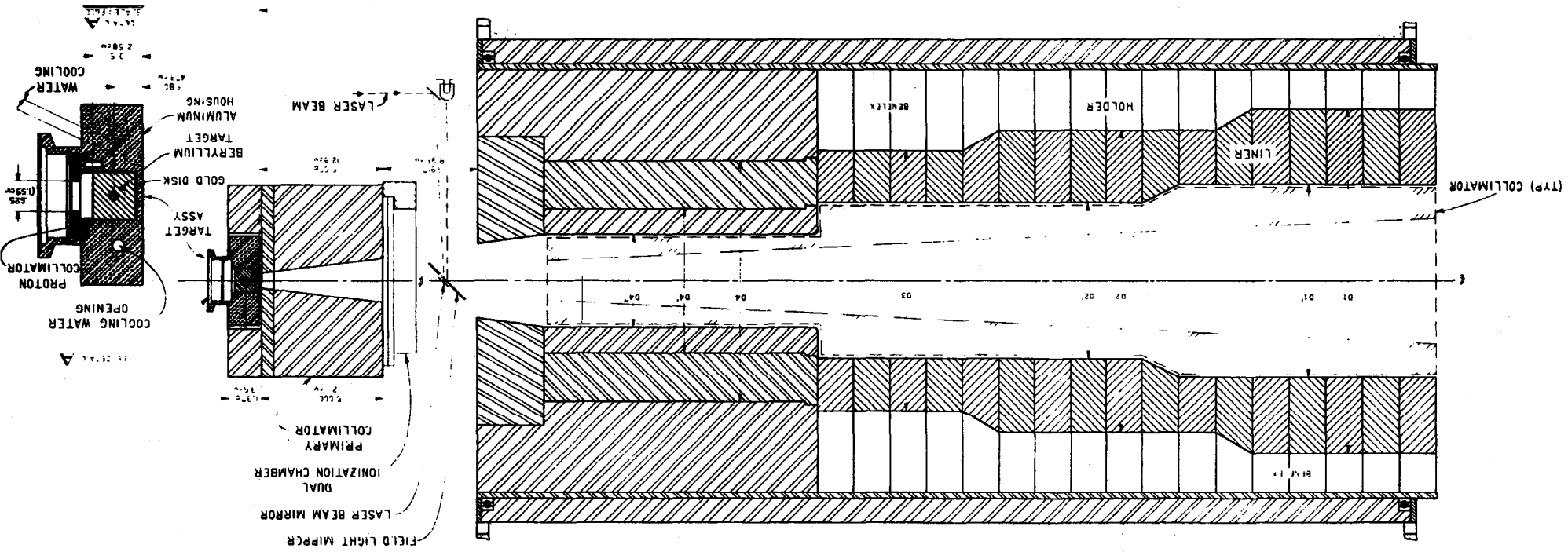


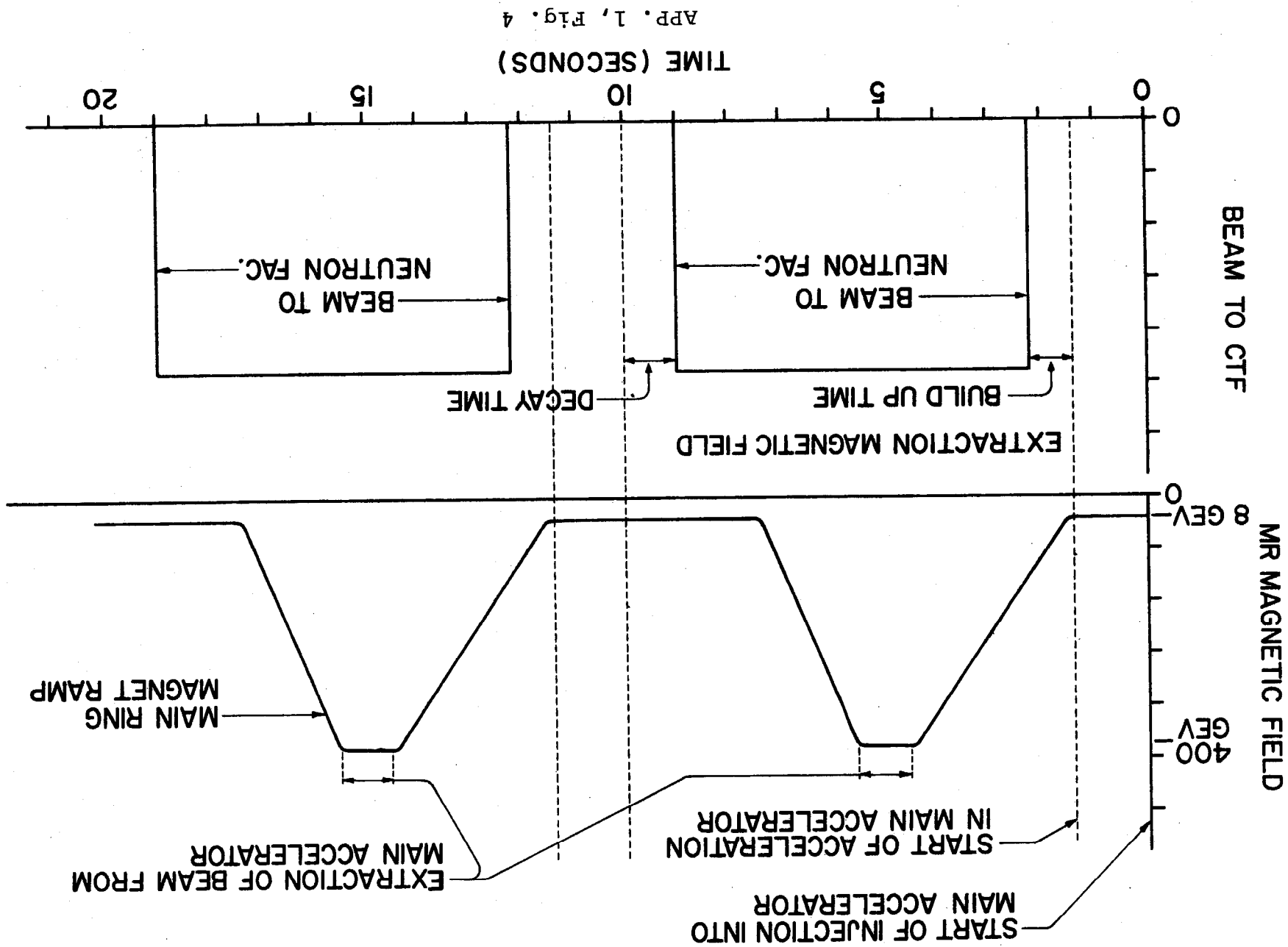
DETAIL **A**  
SCALE : FULL

APP. 1, Fig. 2

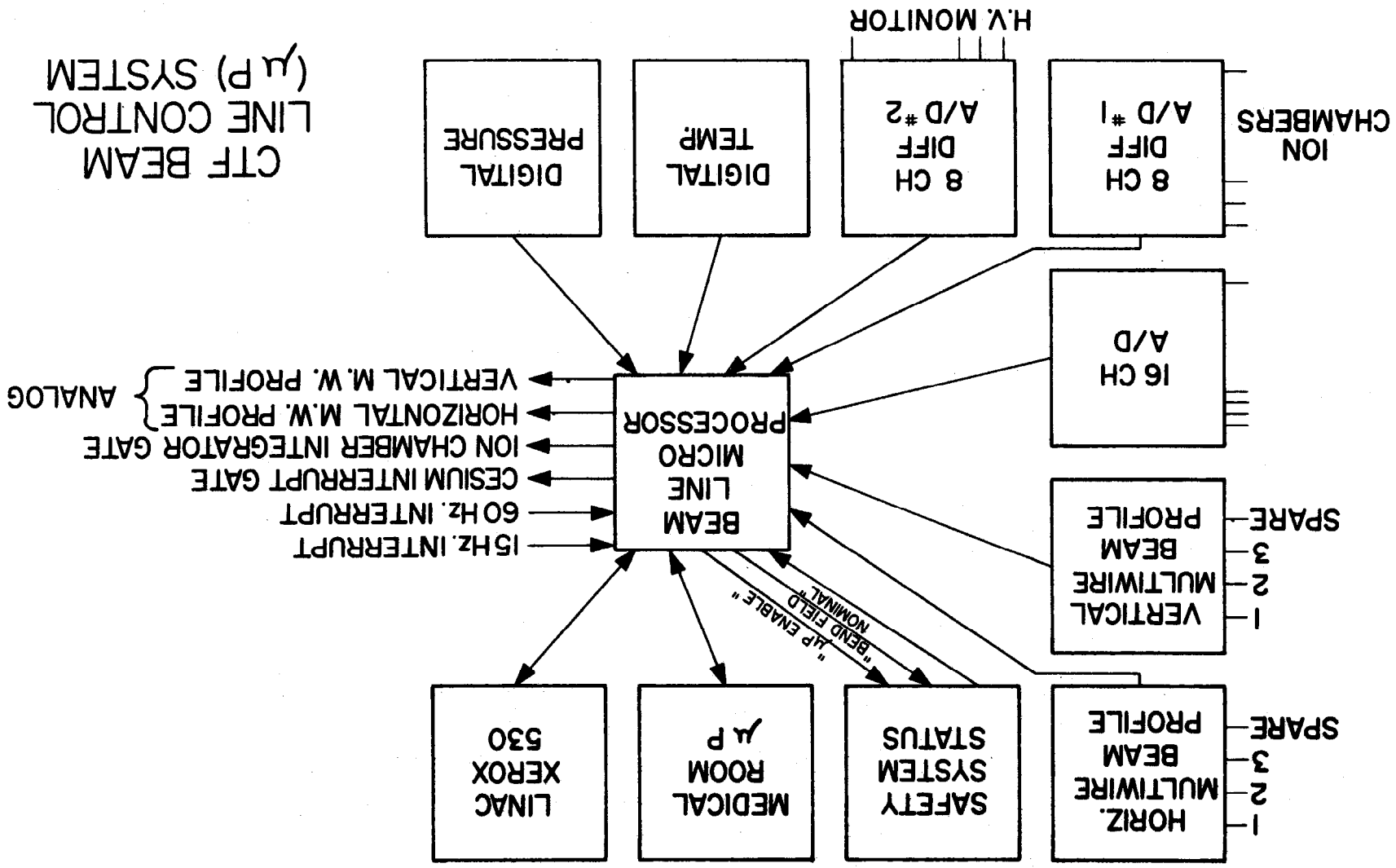


APP. 1, FIG. 3





APP. 1, FIG. 4



## APPENDIX 2

### Microcomputer Calibration System. Display of Outputs

Beam calibration means that a dose of 1 Gray will be absorbed by the mini-phantom, at the location of the center of the one cm<sup>3</sup> ionization chamber, when a dose of 1 Gray is requested by the operator. The "dose outputs" of all collimators are related to the mini-phantom.

In these calibrations both the "Beam Line" (see Appendix 1) and the "Medical" microcomputers are involved.

The beam line microcomputer monitors atmospheric pressure, reads voltages from ionization chamber current integrators, closes and opens reed-relays used to discharge the integrator capacitors and measures time among other functions.

The medical microcomputer measures temperature where needed, sends instructions to the beam line microcomputer and receives information on time, voltages, pressure, etc, from it. This microcomputer makes the necessary arithmetic and displays suitable for utilization by the medical physicists and radiation therapy technologists.

There are two calibration programs of interest for daily therapy: (1) ionization chamber calibration in terms of <sup>60</sup>Co in a <sup>137</sup>Cs source, and (2) neutron beam transmission chamber calibration. The first program transmits directly to the second one the ionization chamber calibration. At midnight, both programs have the calibration constants erased and require a full recalibration procedure.

Although the needed output of each program is only one number, a large number of other variables are also displayed.

Figure 1 shows the ionization chamber calibration page. The word "PREAMP" refers to the combination integrator and output amplifier packed in one small shielded box. CEF x VOUT is the final charge in the capacitor. In practice, the time between two output voltage measurements and their voltage differences are used to calculate dV/dt. "G" in R/C is the measured value. "G-NOM" is a historic value for each chamber used to display with high sensitivity the variations of the chamber calibrations.

Figure 2 shows the neutron beam calibration page. Here "KCOR" is the number used to calibrate the "monitoring units". KNOM is an approximate number used to get the algorithm going. "RAD" stands for "JIGRAD" or rad measured in the mini-phantom. RD/DT is given in units of jigrad/minute.

APP. 2, pg. 2

Figure 3 is the patient treatment page. "\*NSTDTRM\*" allows recording of a portal terminated before scheduled dose is delivered. "SCLR TIME" = time to set in the back-up timer. Quantities in parentheses are nominal values. The adjacent values to the right are the actual values. "BLOCKING" each group of three letters gives block ID and corner location, such as "A" block in Upper Left corner.

The dose required for a particular portal is entered after "REQ'D" by the technologist. When the "GIVEN" dose reaches the requested, the computer switches off the beam and automatically prints the information as shown in Figure 3 for recording purposes.

A7C2=77433402

01/05/79 0649

◆CHAMBER CALIBRATION IN CS-137 (REV 2)

NRUN=5 F=.960080 IC=117T6 PREAMP=6

IC IN @:0632 HOURS POL= 601.8 V

CEF = 2.045NF GAIN= 9.965

FROM 0642 TO 0649 VDUT= 9.603 V

1:T= 24.3 C DT= 89.7 S

P= 1003 MB DVDI= 105.9 MV/S

TPC= 1.017 DVDI-COR= 107.8+/- .00004

G= 3.726E9 R/C G-NOM= 3.686E9 %D= 1.11

DVDI-COR:: 107.8: 107.9: 107.8: 107.7

: 107.8

A7C2=77403E02

01/05/79 0657

◆CHAMBER CALIBRATION IN CS-137 (REV 2)

NRUN=5 F=.960080 IC=117T6 PREAMP=6

IC IN @:0632 HOURS POL= 601.8 V

CEF = 2.045NF GAIN= 9.965

FROM 0650 TO 0657 VDUT= 9.603 V

1:T= 24.3 C DT= 89.72 S

P= 1003 MB DVDI= 105.9 MV/S

TPC= 1.017 DVDI-COR= 107.8+/- .00001

G= 3.728E9 R/C G-NOM= 3.686E9 %D= 1.14

DVDI-COR:: 107.7: 107.8: 107.7: 107.8

: 107.8

APP. 2, Fig. 1

01/05/79 0755

◆ NEUTRON BEAM CALIBRATION

NRUN=5 IC=117 PREAMP=6  
GAIN= 9.965 CEF= 2.045NF G= 3.728E9  
S:T= 25.5 C X:T= 26.6 C P= 1003 MB  
TPC= 1.021 TPC= 1.025 ICHV= 601.8V  
VDM= 9.636V VOUT= 9.624 XCHV= 3002 V  
RUNS FROM 0747 TO 0755 HOURS  
DELV: 9.506 9.502 9.516 9.521 9.531 V  
JGD: 69.38 69.34 69.45 69.49 69.56 RAD  
RQD: 69.8 69.82 69.91 70.07 70.18 RAD  
DT: 1.394 1.394 1.394 1.405 1.399 MIN  
X1: 7258 7261 7269 7285 7295 V  
X2/X1: 1.008 1.008 1.008 1.008 1.008  
QP/XC: .839 .839 .838 .838 .837  
◆RESET AVERAGES & SUMMATIONS  
VX1M= 6.37 V; VX2M= 6.39 V; VQPM= 5.118V  
X2/X1= 1.008 +/- 0 ; .96/1.06  
QP/XC= .838 +/- 0 ; .74/.94  
SDV= 47.57V SJD= 347.2R SRD= 349.7R  
JD/RD= .992 +/- .001 RD/DT= 50.06R/M  
KCDR= 9.311E-3 KNUM=.00938

APP. 2, Fig. 2

```

PATIENT TREATMENT (REV3) 03/10/79 0738
RWD/M: .31 KCUR*1000: 9.345
: CLEAR INTEGRATORS ELPS TIME= .466 MIN
: RESET *NSTDTRM* SCLR TIME= 45.29SEC
PATIENT : SMITH, JOE 10:79-987
FRACTION : 2
PORTAL : RT POST DBL
COLLIMATOR: ( 6X12) X ANG=(350) DEG
BLOCKING : (AUL, , , )
WEDGE : (#1 )# ANG=( 90) DEG
CHAIR : MONOPOLE ANG=(270) DEG
STD OUTPUT REW'D: .117 JIGGY
GIVEN= .114 JIGGY
LIMIT ACTUAL
X1 LIMIT= 7.375 7.313 TX= 27.7 C
X2 LIMIT= 7.375 7.377 P= 986.6 MB
WP LIMIT= 7.375 6.453 TPCX= 1.046
58 DEG 32 DEG XMSN WP/X1 X2/X1
1045 1042 89.64 .881 1.008 A
1046 1043 N
2.124 4.257 T

```

```

0000 0301 0101 007B FFFE (NOM) ACTUAL

```

APP. 2, Fig. 3



APPENDIX 3

Table I  
Results of Inter-Institutional Intercomparisons of  $^{60}\text{Co}$   
Calibration of Ionization Chambers

<u>Intercomparison Site</u>	<u>Date</u>	<u>Visitors</u>	<u>Discrepancy<sup>(1)</sup></u>
NRL	April 1, '77	Fermilab	0.2%
NBS	April 16, '77	Fermilab	Reference
U. of Chicago	June 8, '77	Fermilab	0.3%
MDAH	June 22, '77	Fermilab	0.4%
Fermilab	Aug. 5, '77	NRL U. of Wash.	0.2% 0.2%
GLANTA	Nov. 15, '77	Fermilab	1% <sup>(2)</sup>
Fermilab	Nov. 30, '77	GLANTA NRL	1.2% <sup>(2)</sup> 0.2%
NBS	May 17, '78	Fermilab	0.5%
Fermilab	Jan. 30, '78	MDAH	0.2%
Fermilab	June 17-18, '78	SKI	0.09%

Notes:

- (1) Absolute value of calibration ratio (greater than one) minus one.
- (2) Ionization chamber had an uncertain previous history. The Fermilab calibration was adopted.

After April 16, 1977, chamber calibrations at Fermilab were made by reference to the calibrated  $^{137}\text{Cs}$  source. Before that date, calibrations had been made by comparison to a transfer standard calibrated by NBS.

## APPENDIX 4

### Ionization Chambers

#### Transmission Ionization Chambers

These chambers are contained in an aluminum vessel (1 and 9), which is effectively open to the atmosphere via a leaky gasket (7). The aluminum parallel plates composing the chambers are all equal in shape but of two different thicknesses. The plates marked "10" define sensitive volumes and are thick, 1/32 inch (0.79 mm). The others are thin plates 0.010 inch (0.25 mm). Odd numbered plates, counting from left or right, are polarizing electrodes. A single high voltage connector (5) feeds all polarizing electrodes. The first two even numbered plates from the left (upstream) are connected together and they are known as transmission chamber #1 (X1 in the text). The other two even numbered plates constitute transmission chamber #2 (X2 in the text).

The mean space between plates is 2.9 mm. Alumina insulators<sup>(3)</sup> space the plates among themselves and to the vessel. Three sets of three insulators each are used, one for HV, and two for the collectors.

#### Dosimetry Chambers

Resume of data provided by the manufacturers.

a.) EG&G ionization chambers.

All EG&G chambers used so far at Fermilab have tissue equivalent walls and collectors.

IC-17 Spherical chamber  
Nominal volume 1.0 cm<sup>3</sup>  
ID = 0.50 inch  
Wall thickness = 0.20 inch

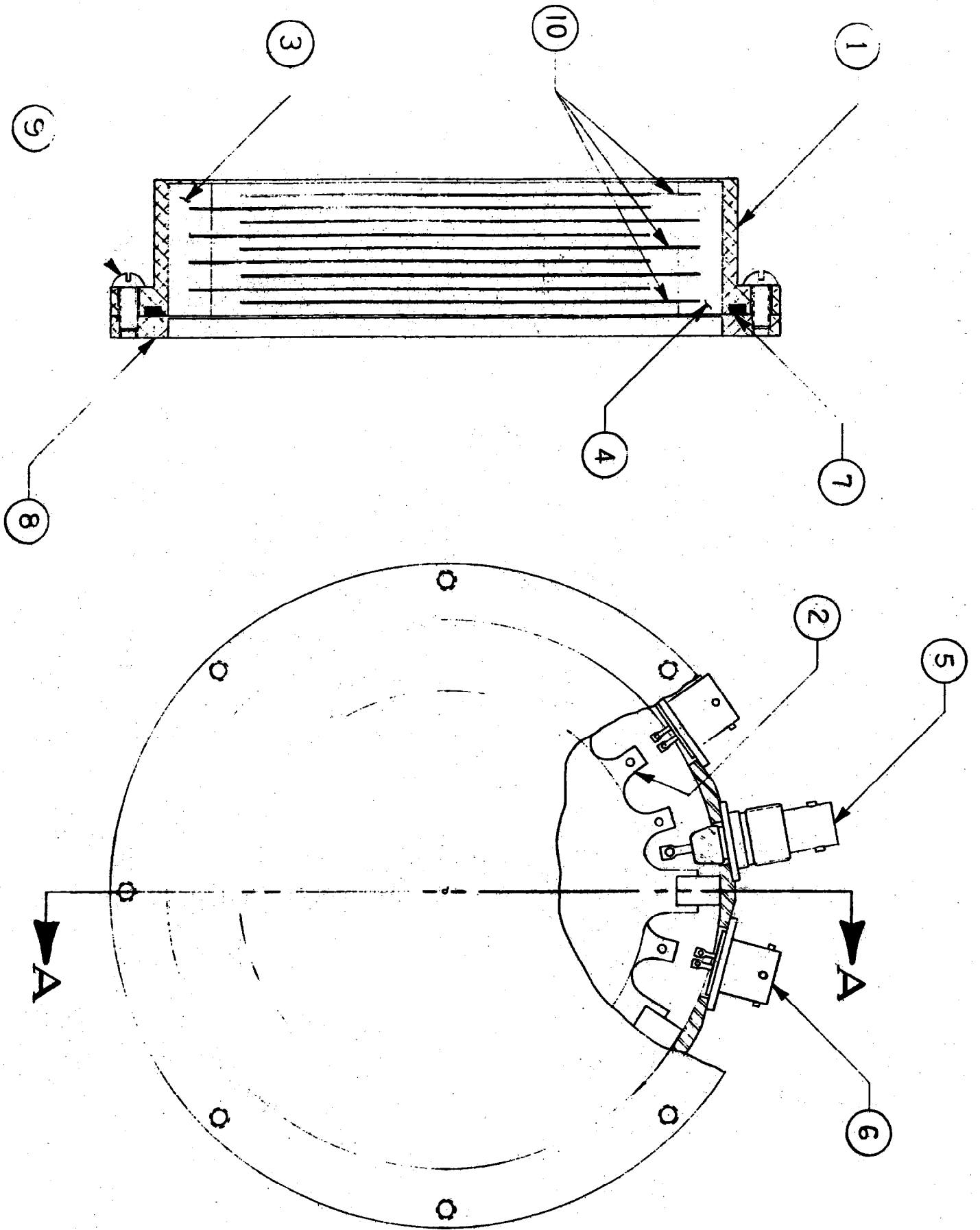
IC-18 Thimble chamber  
Nominal volume 0.1 cm<sup>3</sup> (actually it is closer to 0.14 cm<sup>3</sup>)  
ID = 0.18 inch  
Wall thickness = 0.064 inch

EIC Extrapolation ionization chamber  
Collector diameter = 1 cm

b.) EXRADIN Ionization Chambers

The EXRADIN Chambers used at Fermilab so far have tissue equivalent walls and collectors.

0.5 cc thimble chamber  
Nominal volume = 0.55 cm<sup>3</sup>  
OD = 11 mm  
Wall thickness = 1 mm



APP. 4, Fig. 1 Transmission Chambers

SECRET

## APPENDIX 5

Collimators. Design, taper, materials and activation.

Taper Design. The tapers were designed to use all of the possible neutrons created in the Be target. Therefore, they extrapolate back to a separation of  $2R$  (symbols from Fig. 1) at the upstream end of the target and to a separation  $NW$  at the isoplane, where  $NW$  is the nominal width of the collimator. Hence, the separation  $D_n$  at any distance  $L_n$  from the upstream end of the target for a given  $NW$ , is:

$$(i) \quad D_n = \frac{L_n}{154.3} (NW - 2R) + 2R$$

and the angle of the taper is:

$$(ii) \quad \tan\theta = (\frac{NW}{2} - R)/154.3$$

The two distances of specific interest are  $L_1$  ( $= 32.4$  cm) to the entrance opening and  $L_2$  ( $= 126.2$  cm) to the exit opening of the concrete collimators. The separation  $2R$  was taken as  $1.8$  cm, slightly wider than the actual Ta proton collimator diameter. Thus, the entrance and exit opening dimensions in cm were calculated for a nominal width of  $NW$  cm as:

$$(iii) \quad D_1 = 0.210 (NW - 1.8) + 1.8;$$

$$D_2 = 0.818 (NW - 1.8) + 1.8$$

The list of available collimators is given in Table 1.

The definition of field sizes used in the parametrization algorithms, though, differs from the above. The dimensions used to calculate the equivalent squares, and to normalize the off-axis-ratio distances, use the projection of the exit opening from the center of the Be target. (Fig. 1) Thus the width at a distance  $SSD$  ( $= 153.2 - SID$ ) from the center of the target, for a nominal width  $NW$ , would be:

$$(iv) \quad S = \frac{SSD}{125.1} D_2 = \frac{SSD}{125.1} [0.818 (NW - 1.8) + 1.8]$$

It follows that the width at the isoplane from this definition is:

$$(v) \quad W = \frac{153.2}{125.1} [0.818 (NW - 1.8) + 1.8] = 1.002 (NW - 1.8) + 2.2 \\ \approx NW + 0.4$$



SUBJECT

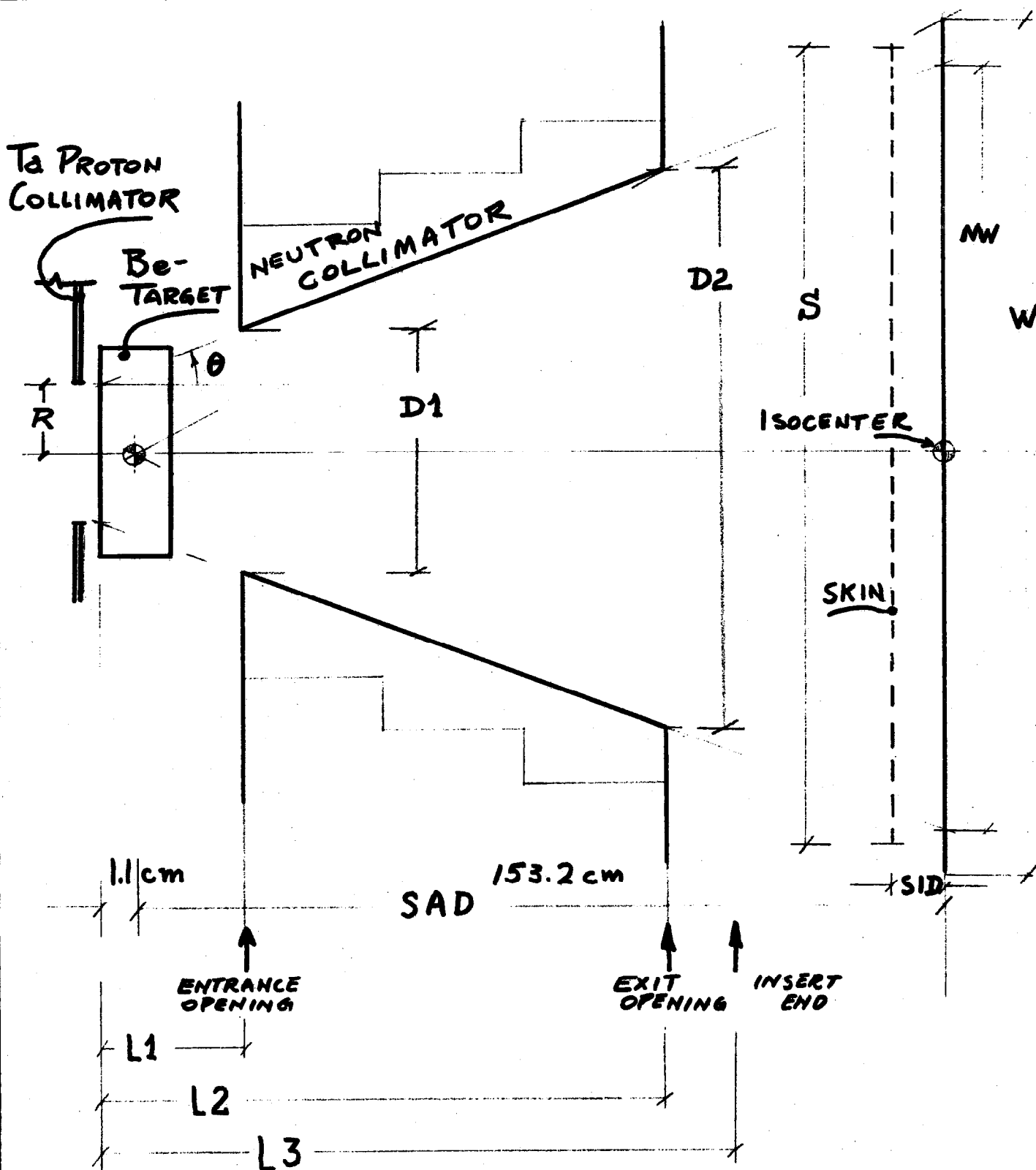
NEUTRON BEAM COLLIMATOR  
DEFINITION OF PARAMETERS

NAME

DATE

1/11/79

REVISION DATE



Appendix 5 Fig. 1

APPENDIX 5

Table 1

LIST OF COLLIMATORS AVAILABLE AT FERMILAB C.T.F.

(Nominal sizes at Isoplane)

1.9 $\emptyset$ circle	8 x 20*	Large size form
3 x 3	9 x 16	10 x 20
5 x 7	10 x 10	20 x 20
6 x 6	10 x 12	25 x 25
6 x 8	10 x 15*	30 x 30
6 x 10	12 x 12	
6 x 12	12 x 15	
7 x 20*	14 x 18	
8 x 8	15 x 15	
8 x 10	16 x 16@	
8 x 12		
8 x 15		

Notes: Large size forms need a crane to change

\* Midline shielding (2 cm. wide) available

@ Octagonal: corners cut ~ 2 cm. (for ca cervix)

APPENDIX 5

Table 2

Physical characteristics of polyethelene concrete.

(a) Composition, by weight:

Portland cement : 50%

Polyethelene Pellets (1/8") : 20%

Water : sufficient to reach 100%

(b) Density of polyethelene concrete =  $1.6 \text{ g cm}^{-3}$

(c) Broad beam absorption coefficient for Fermilab neutrons (from  $e^{-\lambda x}$ ).  $\lambda = 0.076 \text{ cm}^{-1}$

(d) Transmission through 94.2 cm of collimator length =  $e^{-94.2\lambda} = 0.0008 = 0.08\%$

(e) Weight range for small collimators: 14.0 kg - 28.5 kg

APPENDIX 5

Table 3

Main spallation products from upstream end of collimator,  
corrected to 24 hr. after last irradiation.

<sup>7</sup> Be	5.0	nCi/g
<sup>24</sup> Na	4.4	"
<sup>47</sup> Se	2.6	"
<sup>54</sup> Mn	0.9	"
<sup>43</sup> K	0.7	"
<sup>51</sup> Cr	0.5	"
<sup>47</sup> Ca	0.4	"
<sup>46</sup> Se	0.2	"
<sup>22</sup> Na	0.2	"
<sup>52</sup> Mn	0.1	"
<sup>57</sup> Co	0.01	"

Remnant radioactivity at contact 24 hr. after irradiation  
≈ 10 mR/hr. at upstream end of collimator.



## APPENDIX 6

### Central Axis Depth Dose. Parametrization.

The central axis dose can be separated into a product between geometrical and nuclear interaction factors:

$$(i) \quad CADD (coll, SSD, z) = K \left( \frac{153.2}{SSD+z} \right)^2 G(ESQ, z)$$

where K is a normalizing factor and ESQ, the equivalent square at the surface, can be derived from the width  $S_W$  and height  $S_H$  of the field at the surface using the formula:

$$(ii) \quad ESQ = 2 \frac{S_W * S_H}{S_W + S_H} = 4 \frac{\text{Area}}{\text{Perimeter}}$$

$S_W$  and  $S_H$  are defined as in equation (iv) of Appendix 5. The form of the function G is:

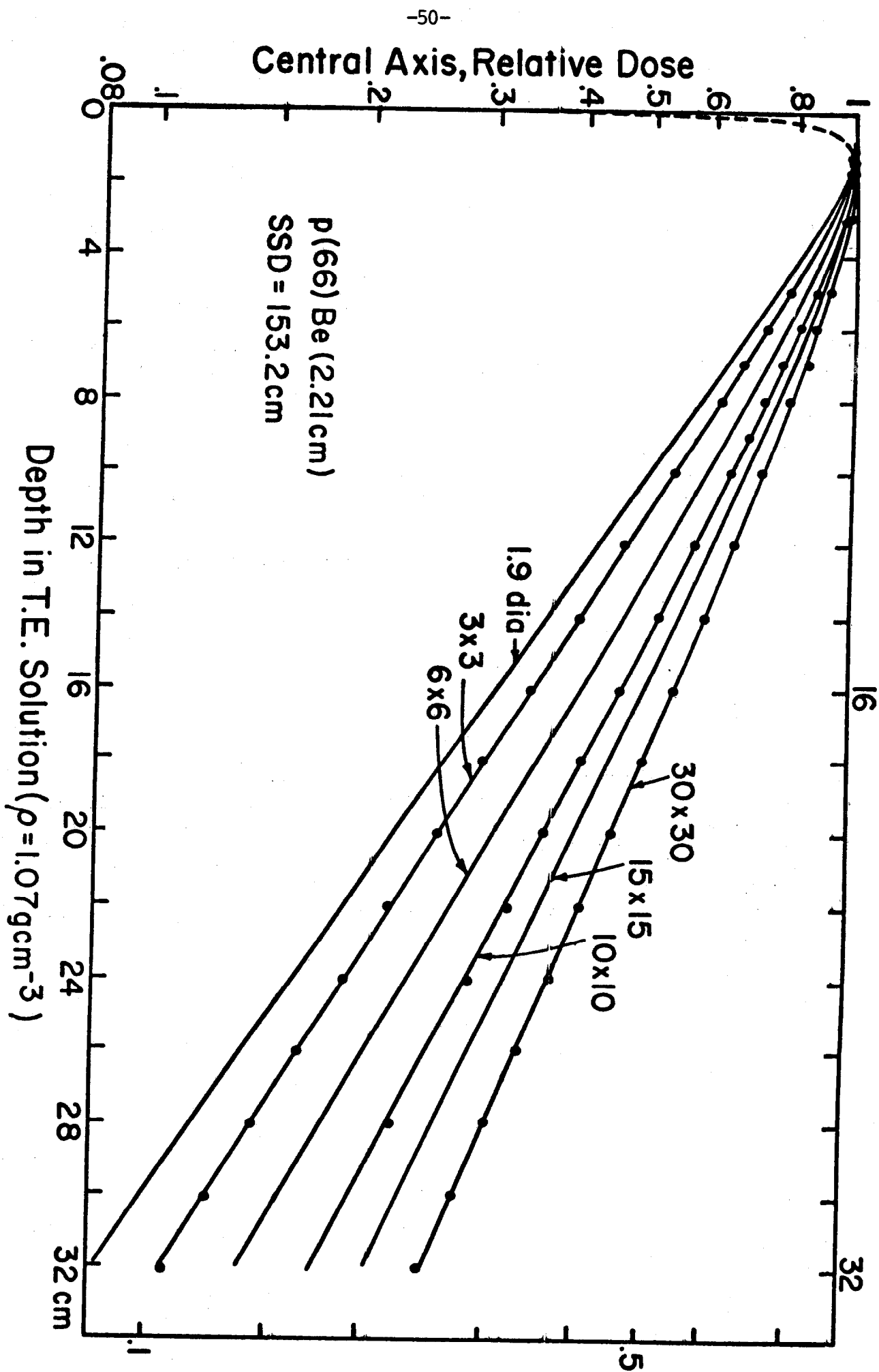
$$(iii) \quad G(ESQ, z) = \{1 - U2 * \exp[-(z/U3) ** U4]\} * \exp(-z/U1)$$

where the dependence on ESQ is implicit in the variation of the parameters:

$$\begin{aligned} (iv) \quad U1 &= 10.0352 * (ESQ ** 0.27762) \\ U2 &= 0.74289 \\ U3 &= 0.55896 + 0.65750 * \ln(ESQ) \\ U4 &= 0.240388 * \exp(-0.0077458 * ESQ) \end{aligned}$$

The goodness of fit of this algorithm can be seen in Fig. 1, where the dots represent the observed depth doses and the lines the fitted algorithm, all doses having been normalized to 1.0 at the depth of maximum build-up.

The build-up curves for the 6 x 6 cm<sup>2</sup> and the 15 x 15 cm<sup>2</sup> collimators, normalized to 1.0 at maximum, are shown in Fig. 2.





FERMILAB  
ENGINEERING NOTE

SECTION

PROJECT

SERIAL-CATEGORY

PAGE

SUBJECT

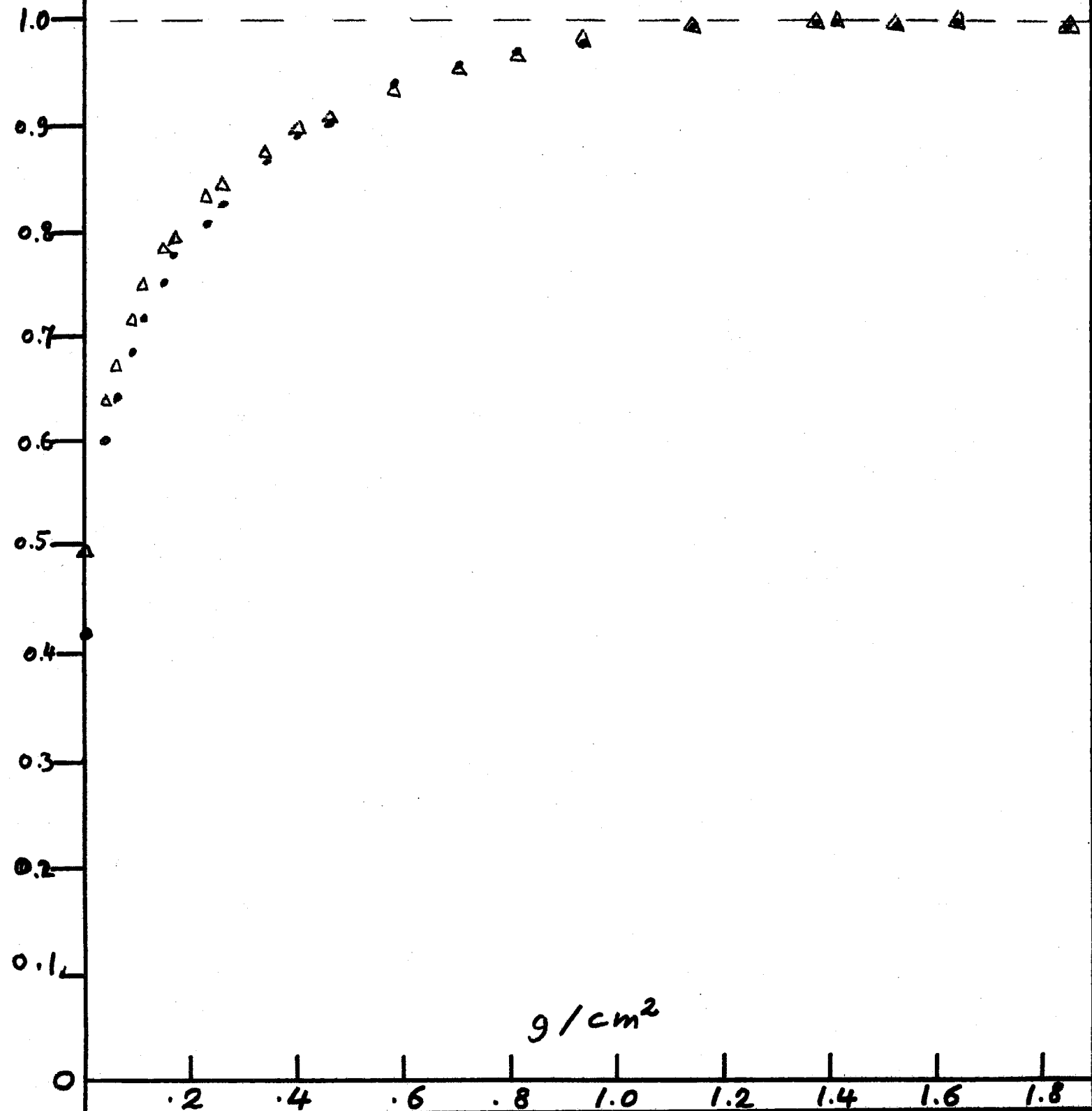
APP. 6, Fig. 2 (Build-up)

NAME

DATE

REVISION DATE

•  $6 \times 6 \text{ cm}^2$  collimator  
 $\Delta$   $15 \times 15 \text{ cm}^2$  "



## APPENDIX 7

### Tissue Standard Ratios. Parametrization.

#### A Reference TSR parametrization.

To characterize a given collimator, its equivalent square at the isoplane (SAD = 153.2 cm) was used. Following from equation (ii) of Appendix 6,

$$(i) \quad ESQ\phi = 2 \frac{W \cdot H}{W + H}$$

where W and H are the width and height of the field at the isoplane as defined in equation (v) of Appendix 5. This parameter is adequate for both squares and rectangles. It follows from these definitions that,

$$(ii) \quad ESQ = \left( \frac{SSD}{153.2} \right) * ESQ\phi$$

It is also convenient to express the equivalent square at the surface for the reference SSD of 143.2 cm as:

$$(iii) \quad ESQR = \left( \frac{143.2}{153.2} \right) * ESQ\phi$$

The measured values of reference TSR at a source-skin distance (SSD) of 143.2 cm and at a depth (z) of 10 cm (i.e., at the isocenter), were parametrized using  $ESQ\phi$  as follows:

$$(iv) \quad \begin{aligned} TSR(coll, 143.2, 10) &= TSR(ESQ\phi, 143.2, 10) = \\ &= 0.45417 * ESQ\phi^{0.33193} \end{aligned}$$

The observed and fitted values of  $TSR(ESQ\phi, 143.2, 10)$  for the original set of collimators are shown in Table 1.

#### B. SSD dependence parametrization.

Using the following formalism to analyze TSR measured at different SSD and depths z:

$$(v) \quad \begin{aligned} TSR(coll, SSD, z) &= \\ &= TSR(ESQ\phi, 143.2, 10) F(SSD) \left( \frac{153.2}{SSD+z} \right)^2 \frac{G(ESQ, z)}{G(ESQR, 10)} \end{aligned}$$

the function  $F(SSD)$  was evaluated in the form,

$$(vi) \quad F(SSD) = \left( \frac{SSD}{143.2} \right)^y$$

The value of y was small and similar for all collimators studied and its mean value of  $y = -0.06176$  was adopted.

APP. 7, pg. 2

C. TSR Tables.

Using equation (v) together with the algorithms developed for each function in it, tables of TSR were generated for each available collimator, ranging in SSD from 133.2 to 153.2 cm and in depths from 0 to 30 cm. A summary table for all collimators for the special case  $SSD+z=\text{constant}=153.2$ , useful in isocentric set-ups, is shown in Table 2. The rows are labelled by Skin-Isocenter Distance  $SID=153.2-SSD$ , and thus, for isocentric treatments  $SID=z$  in all cases.

VALUES FOR NEW JIG 17SEP77, VALUES ARE MEANS OF THREE DIFF. GROUPS:

LONG-TIME(=27JUL 77), 16APR77 BOTH X 2,123, AND 16SEP77 WITH NEW JIG,

1  $AM10 = .31293E+01 * ESQ0 + .65441E+00$  CERR: 0,9936

2  $AM10 = .32368E+00 * LN(ESQ0) + .23415E+00$  CERR: 0,9972

3  $AM10 = .70071E+00 * EXP(.31834E-01 * ESQ0)$  CERR: 0,9870

4  $AM10 = .45417E+00 * (ESQ0)** .33193E+00$  CERR: 0,9986

CORRELATION CHOSEN: 4

W	H	OBSERV	FITTED	% DIFF
5X 7		,8352	,8347	=0,1
6X 6		,8392	,8415	0,3
6X 8		,8752	,8777	0,3
6X10		,9034	,9034	=0,0
8X 8		,9297	,9210	=0,9
8X10		,9464	,9525	0,6
8X12		,9828	,9764	=0,7
10X10		,9895	,9887	=0,1
7X20		1,0078	1,0030	=0,5
8X15		1,0072	1,0033	=0,4
10X12		1,0100	1,0167	0,7
10X15		1,0432	1,0486	0,5
12X12		1,0421	1,0481	0,6
15X15		1,1244	1,1263	0,2
14X18		1,1502	1,1443	=0,5

# TISSUE STANDARD RATIOS (RAD/ JIB RAD) AT ISOCENTER

SI0.2

NOMINAL COLLIMATOR SIZES (CM)

6-JAN-78

(CM) 3X 3 5X 7 6X 6 6X 8 6X1F 7x20 8X 8 8X10 8X12 6X15 9X10 10X10 10X12 10X15 12X12 12X15 14X14 15X15 16X16 24x24

6x12

8x20

10x20

0	1.044	1.165	1.171	1.231	1.222	1.307	1.237	1.264	1.284	1.307	1.335	1.295	1.319	1.347	1.346	1.378	1.431	1.415	1.437	1.585
1	1.056	1.181	1.186	1.217	1.236	1.325	1.254	1.281	1.301	1.322	1.323	1.332	1.357	1.365	1.364	1.397	1.451	1.434	1.456	1.605
2	1.072	1.197	1.202	1.233	1.255	1.342	1.270	1.295	1.319	1.343	1.331	1.350	1.383	1.383	1.383	1.415	1.470	1.454	1.475	1.620
3	1.033	1.166	1.172	1.204	1.228	1.319	1.244	1.272	1.294	1.319	1.300	1.302	1.331	1.361	1.362	1.394	1.450	1.433	1.456	1.611
4	1.084	1.124	1.132	1.164	1.188	1.281	1.224	1.234	1.256	1.282	1.312	1.290	1.322	1.324	1.329	1.359	1.416	1.399	1.422	1.579
5	1.032	1.076	1.083	1.118	1.142	1.236	1.159	1.189	1.212	1.238	1.209	1.224	1.251	1.282	1.272	1.317	1.375	1.358	1.381	1.545
6	1.080	1.027	1.034	1.069	1.094	1.192	1.112	1.142	1.166	1.192	1.144	1.178	1.202	1.237	1.246	1.272	1.331	1.313	1.336	1.497
7	1.028	1.075	1.085	1.120	1.146	1.246	1.144	1.163	1.194	1.118	1.145	1.176	1.135	1.158	1.190	1.145	1.225	1.205	1.227	1.432
8	1.077	1.029	1.036	1.072	1.097	1.197	1.115	1.146	1.170	1.197	1.149	1.182	1.116	1.142	1.142	1.178	1.238	1.220	1.243	1.405
9	1.029	1.081	1.088	1.124	1.150	1.249	1.149	1.167	1.199	1.123	1.150	1.182	1.135	1.158	1.190	1.145	1.225	1.205	1.227	1.432
10	1.082	1.035	1.042	1.078	1.103	1.202	1.121	1.152	1.176	1.100	1.125	1.156	1.109	1.132	1.164	1.114	1.194	1.176	1.199	1.402
11	1.036	1.079	1.086	1.122	1.147	1.246	1.146	1.164	1.196	1.120	1.146	1.178	1.130	1.153	1.185	1.136	1.216	1.198	1.221	1.406
12	1.096	1.047	1.054	1.090	1.115	1.214	1.134	1.162	1.186	1.110	1.136	1.168	1.120	1.143	1.175	1.126	1.206	1.188	1.211	1.421
13	1.057	1.105	1.112	1.148	1.173	1.272	1.172	1.190	1.222	1.146	1.172	1.204	1.156	1.179	1.211	1.162	1.242	1.224	1.247	1.455
14	1.019	1.066	1.073	1.109	1.134	1.233	1.133	1.151	1.183	1.107	1.133	1.165	1.117	1.140	1.172	1.123	1.203	1.185	1.208	1.432
15	1.084	1.036	1.043	1.079	1.104	1.203	1.123	1.151	1.175	1.100	1.126	1.158	1.110	1.133	1.165	1.116	1.196	1.178	1.201	1.456
16	1.045	1.092	1.099	1.135	1.160	1.259	1.159	1.177	1.209	1.133	1.159	1.191	1.143	1.166	1.198	1.149	1.229	1.211	1.234	1.485
17	1.020	1.068	1.075	1.111	1.136	1.235	1.135	1.153	1.185	1.109	1.135	1.167	1.119	1.142	1.174	1.125	1.205	1.187	1.210	1.455
18	1.091	1.042	1.049	1.085	1.110	1.209	1.129	1.157	1.181	1.105	1.131	1.163	1.115	1.138	1.170	1.121	1.201	1.183	1.206	1.480
19	1.053	1.100	1.107	1.143	1.168	1.267	1.167	1.185	1.217	1.141	1.167	1.199	1.151	1.174	1.206	1.157	1.237	1.219	1.242	1.515
20	1.038	1.085	1.092	1.128	1.153	1.252	1.152	1.170	1.202	1.126	1.152	1.184	1.136	1.159	1.191	1.142	1.222	1.204	1.227	1.500

## APPENDIX 8

### Off-axis Ratios. Parametrization.

The off-axis ratio (OAR) for a collimator of width  $W$  at the isoplane (see equation (v) of App. 5) at a given SSD and depth  $z$  was reproduced by a smooth multifunction, multiparameter algorithm.

First, the nominal width of the field  $XN$  at the plane of interest is calculated from:

$$(i) \quad XN = \left( \frac{SSD+z}{153.2} \right) * W$$

and then a normalized set of coordinates is defined as:

$$(ii) \quad y = \left| \frac{x}{XN} \right|$$

where  $x$  is the actual distance from the central axis. The OAR function shown in Fig. 1 is then divided into four separate functions,  $R_1$  to  $R_4$ , constrained to match in value and derivative at three match points,  $y = BP$ ,  $y = 1$  and  $y = U3$ . The forms of the functions  $R$  are as follows:

$$(iii) \quad R_1 = \text{EXP}[-U2*(y**U1)] \quad : \text{for } 0 \leq y \leq BP$$

$$R_2 = A \left\{ 1 - B * \text{EXP} \left[ -U5 * \left( \frac{1-y}{y} \right) \right] \right\} \quad : \text{for } BP \leq y \leq 1$$

$$R_3 = M * \text{EXP}[-L*(y+U4-1) **U7] \quad : \text{for } 1 \leq y \leq U3$$

$$R_4 = Q * \text{EXP}[-S*(y+U6-U3)**U8] \quad : \text{for } U3 \leq y \leq \infty$$

The values of  $A$ ,  $B$ ,  $M$ ,  $L$ ,  $Q$  and  $S$  are completely defined in terms of  $U$ 's by the requirements that the functions and their derivatives are matched at the match points. The parameters  $U1$  to  $U8$  and  $BP$  are correlated with field width  $W$  and depth  $z$  to fit all available data:

$$(iv) \quad U1 = (4.437-0.0862W)-(0.0605-0.0002W)*z$$

$$U2 = 0.09686+(0.00526+0.0041W)*\ln(z)$$

$$U3 = (1.098+0.011W)+(0.00376+0.000674W)*z$$

$$U4 = 0.1$$

$$U5 = (0.4182W+23.8)-(0.783+0.174W)*\ln(z)$$

$$U6 = (0.113-0.00923W)+(0.0346-0.00107W)*z$$



APP. 8, pg. 2

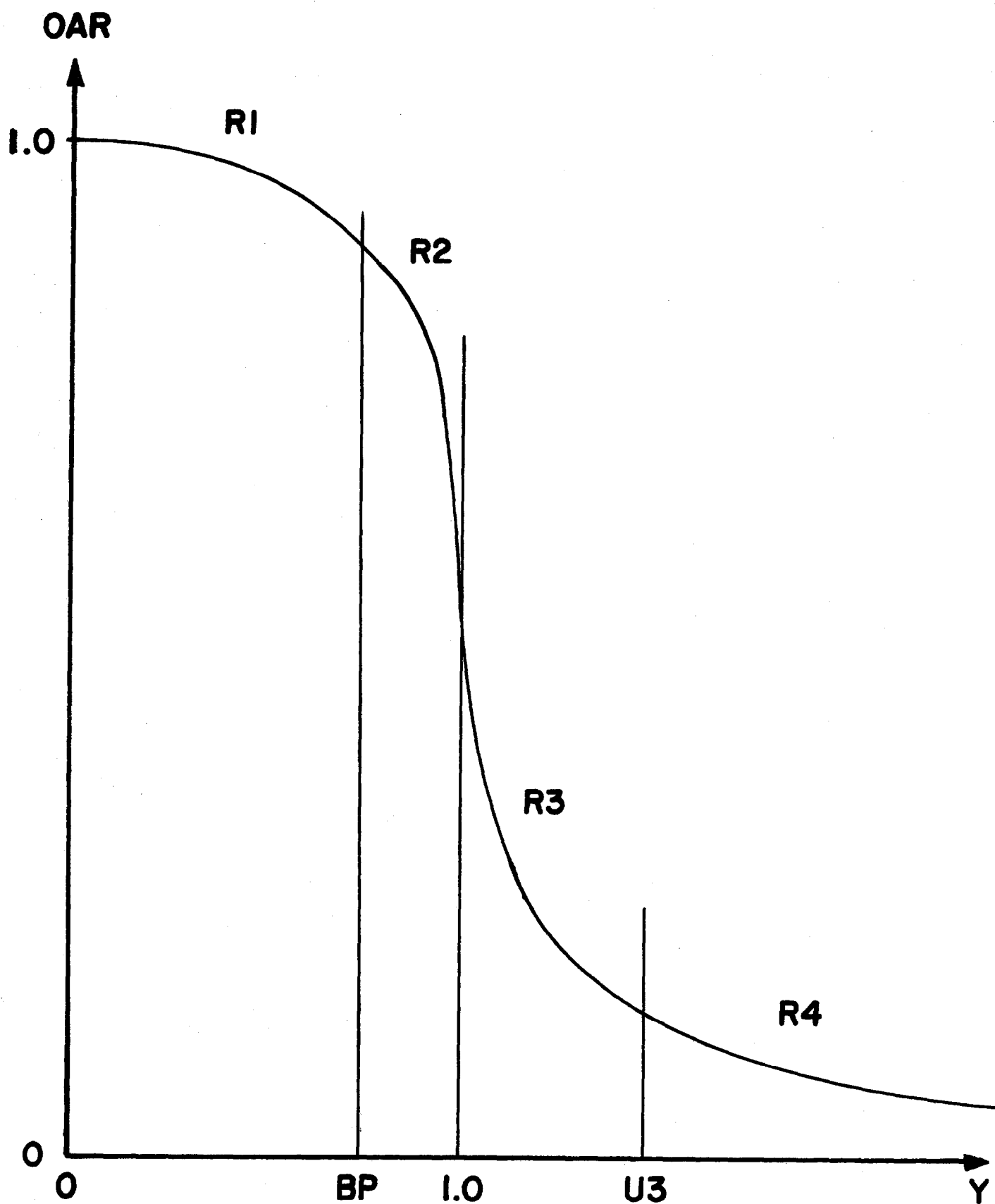
$$U7 = 0.0445 - 0.00179W$$

$$U8 = (0.0205W - 0.0322) + 0.01 * z$$

$$BP = 0.882$$

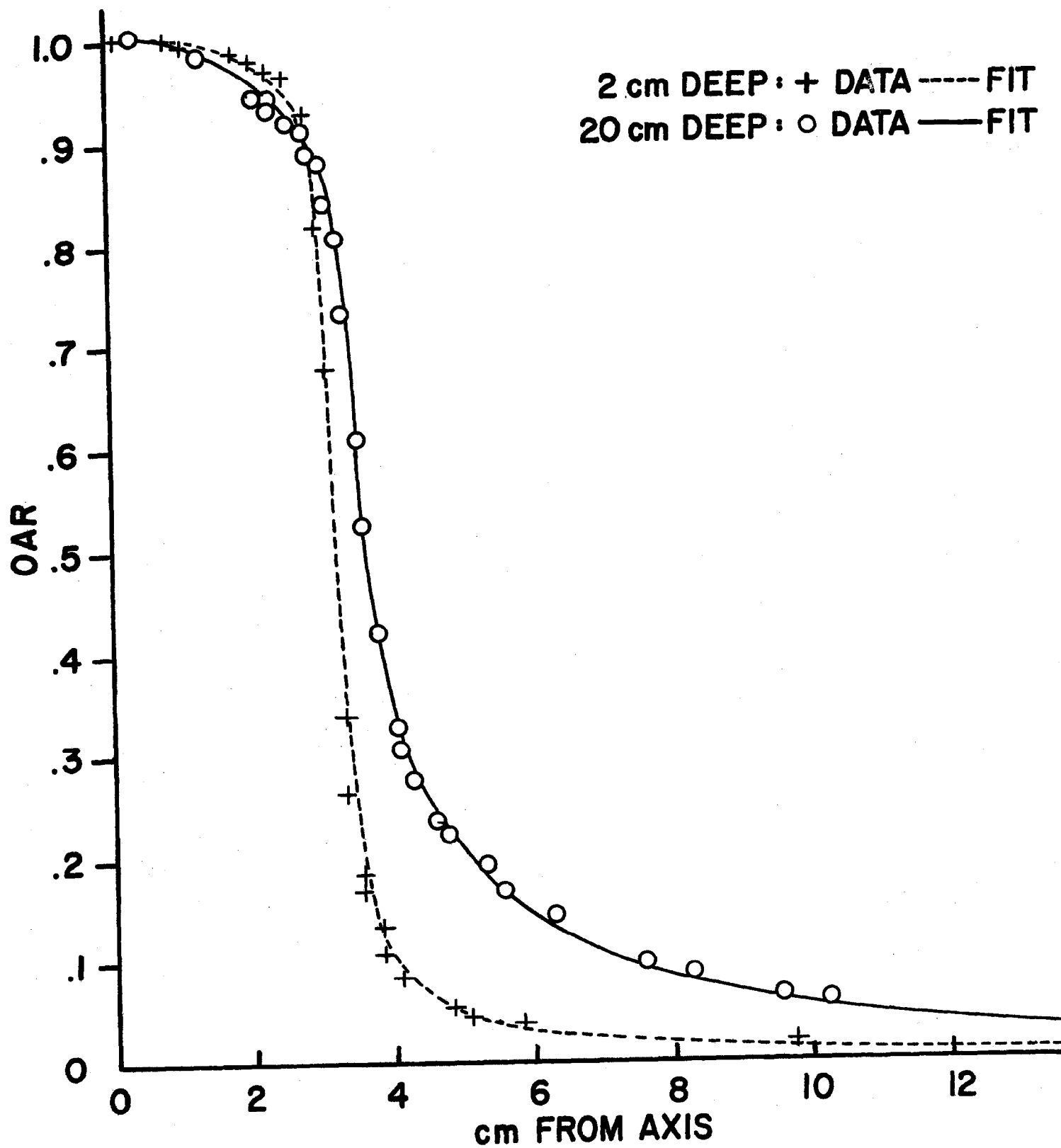
Some typical fits of this algorithm to the data can be seen in Figs. 2 to 4.

APP. 8, Fig. 1

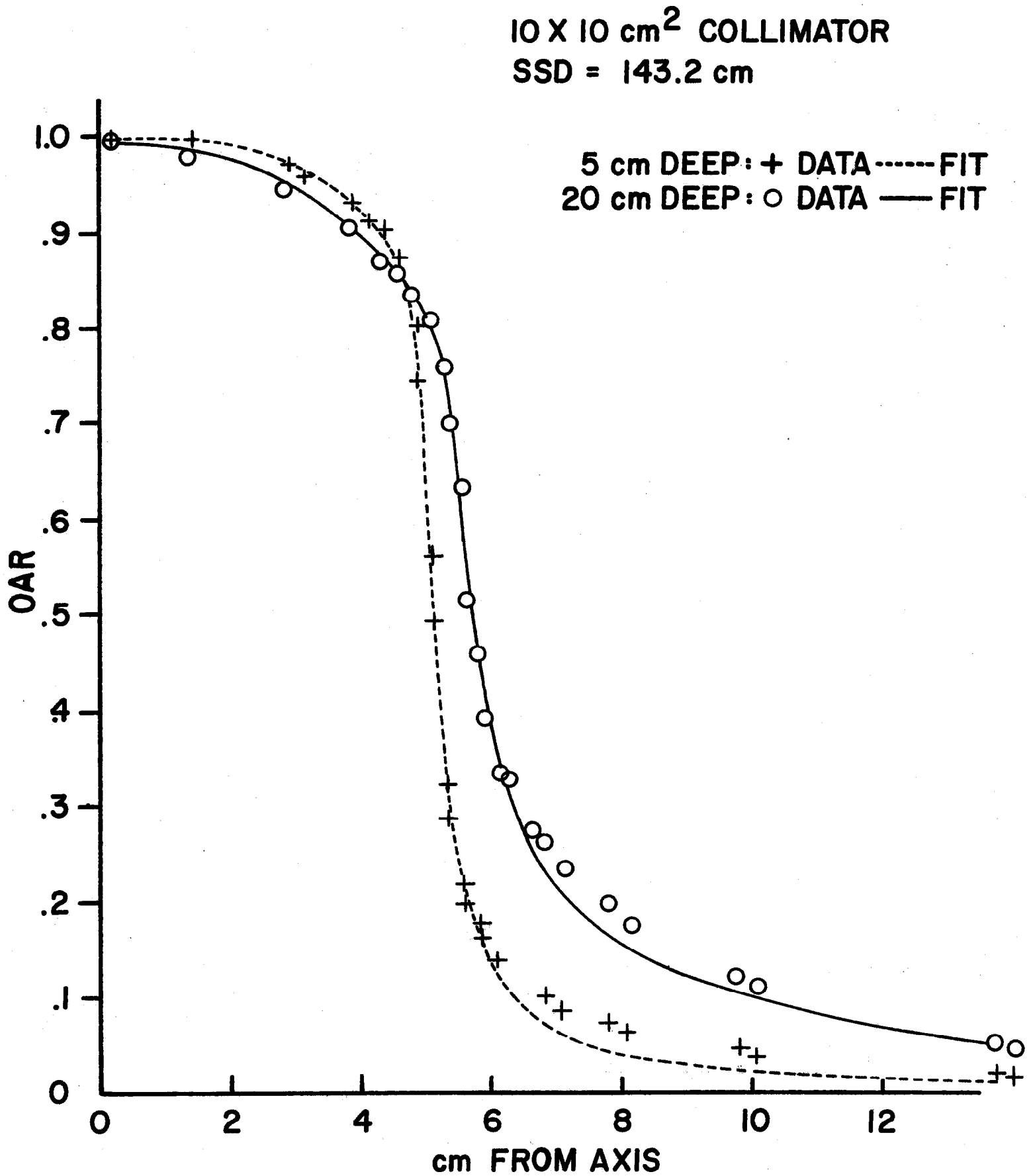


APP. 8, Fig. 2

6 X 6 cm<sup>2</sup> COLLIMATOR  
SSD = 153.2 cm

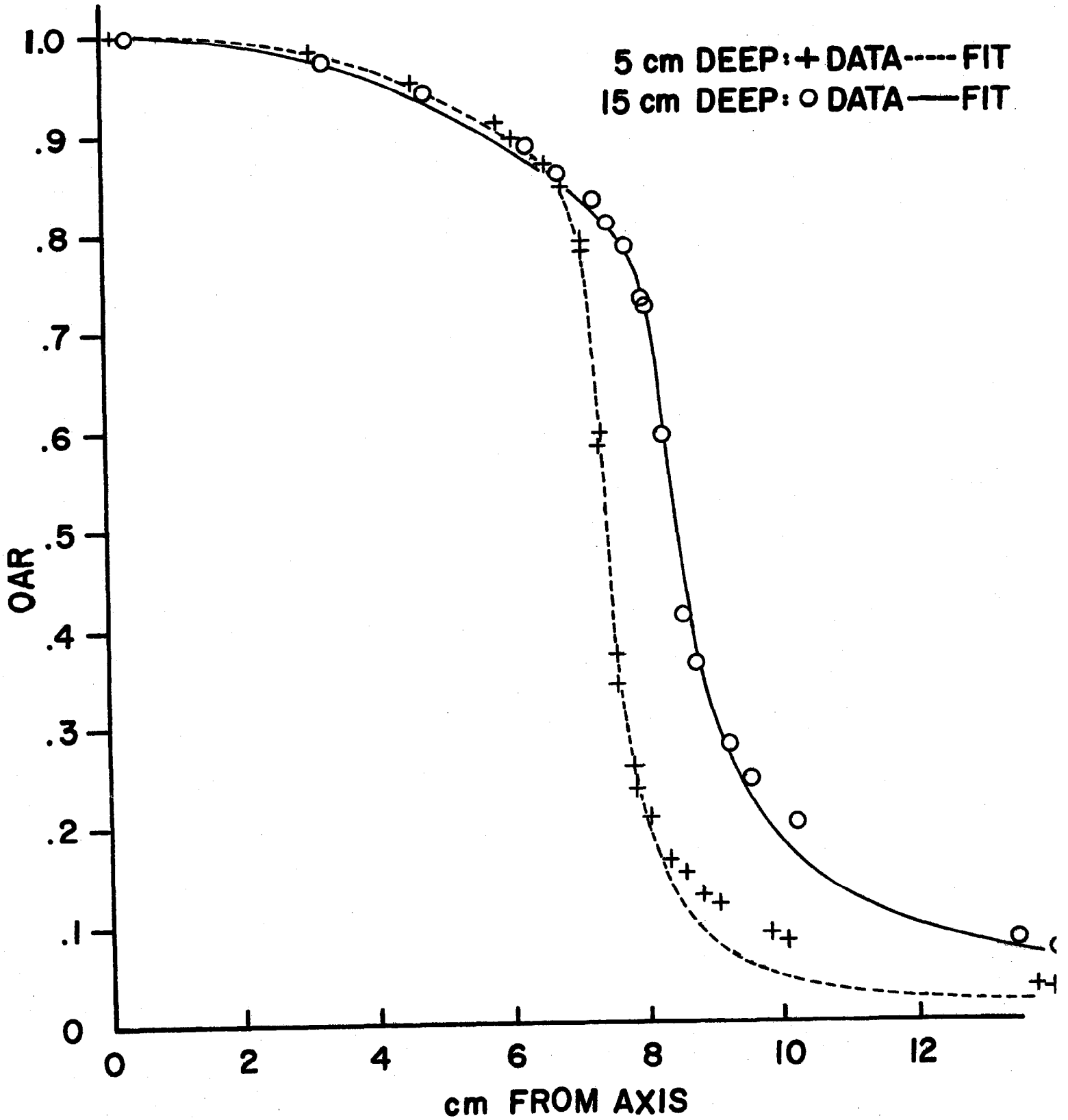


APP. 8, Fig. 3



APP. 8, Fig. 4

15 X 15 cm<sup>2</sup> COLLIMATOR  
SSD = 153.2 cm



# APPENDIX 9

## Wedge filter. Parametrization.

A wedge filter, used in patient treatment to achieve more uniform distribution in many beam combinations, was made out of Teflon (PTFE) with an actual angle of 31°.

When used in front of a collimator, the output on the central axis is reduced by an amount called the wedge factor WF. This factor varies with the equivalent square of the collimator to some extent. Two such wedges of different dimensions but equal angle are employed, one covering field sizes up to 10 cm in either direction, and one covering up to 15 cm. Their absorption factors can be calculated by the formulae:

$$(i) \quad WF = 0.696 + 0.00565 \cdot ESQ\phi \quad (\text{small wedge})$$

$$= 0.598 + 0.00700 \cdot ESQ\phi \quad (\text{large wedge})$$

where  $ESQ\phi$  is the equivalent square at the isoplane (equation (i) of App. 7).

The purpose of the wedge filter is to change the dose distribution asymmetrically about the central axis. Thus, its influence on the off-axis ratios can be reproduced by an additional function:

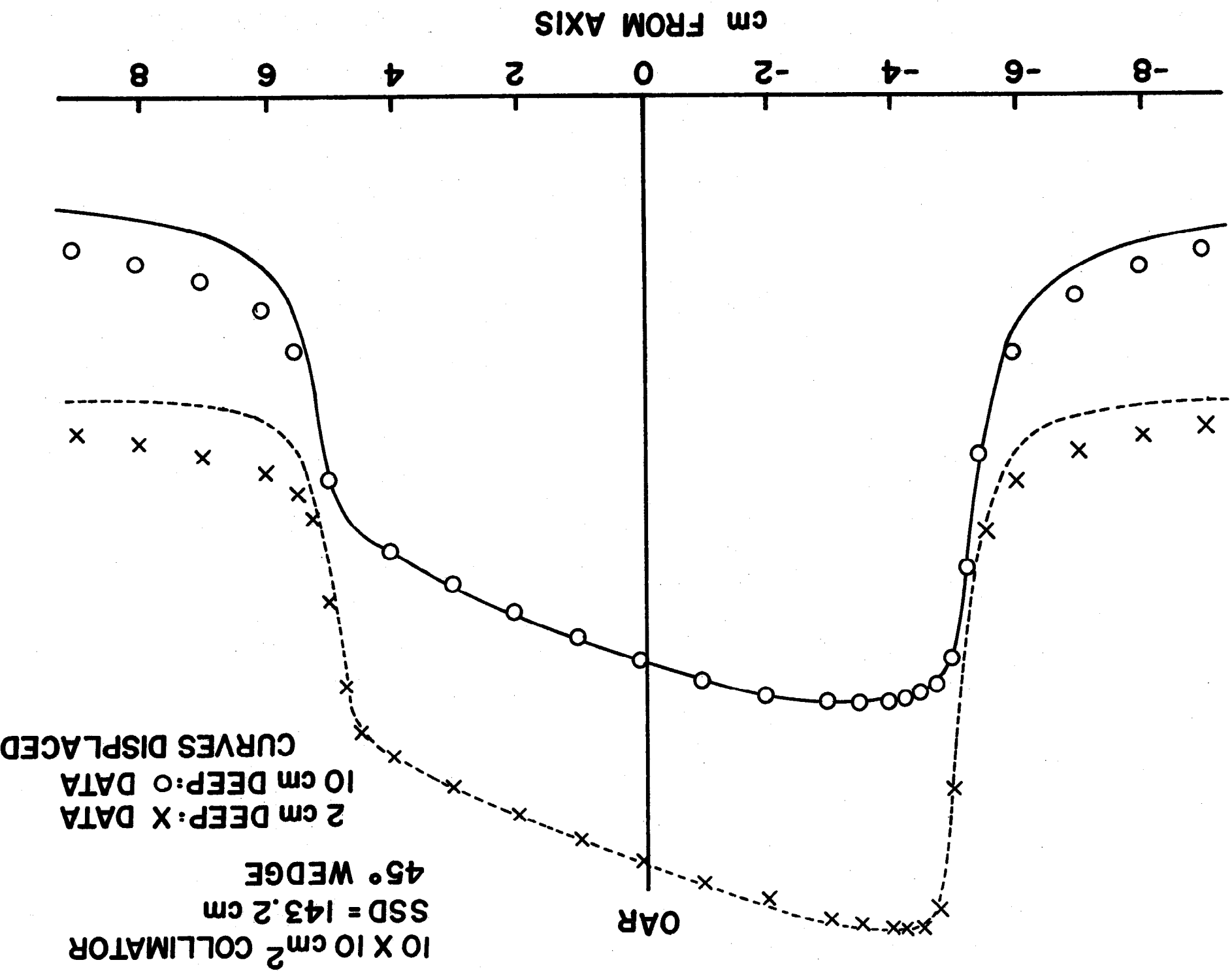
$$(ii) \quad WOAR = OAR \cdot \exp \left[ -P x \left( \frac{153.2}{SSD+z} \right) \right]$$

where the factor  $P$  is dependent on field size  $W$  and depth  $z$  as follows:

$$(iii) \quad P = (0.0751 - 0.00255W) + (0.0118 - 0.0008W) \cdot \ln(z)$$

Some typical fits of this algorithm to the data are shown in Fig. 1.

APP. 9, Fig. 1



## APPENDIX 10

### Alignment Systems and Checks

Figure 1 shows an elevation view of the treatment room, with the relative position of the X-ray isocenter and neutron isocenter clearly displayed.

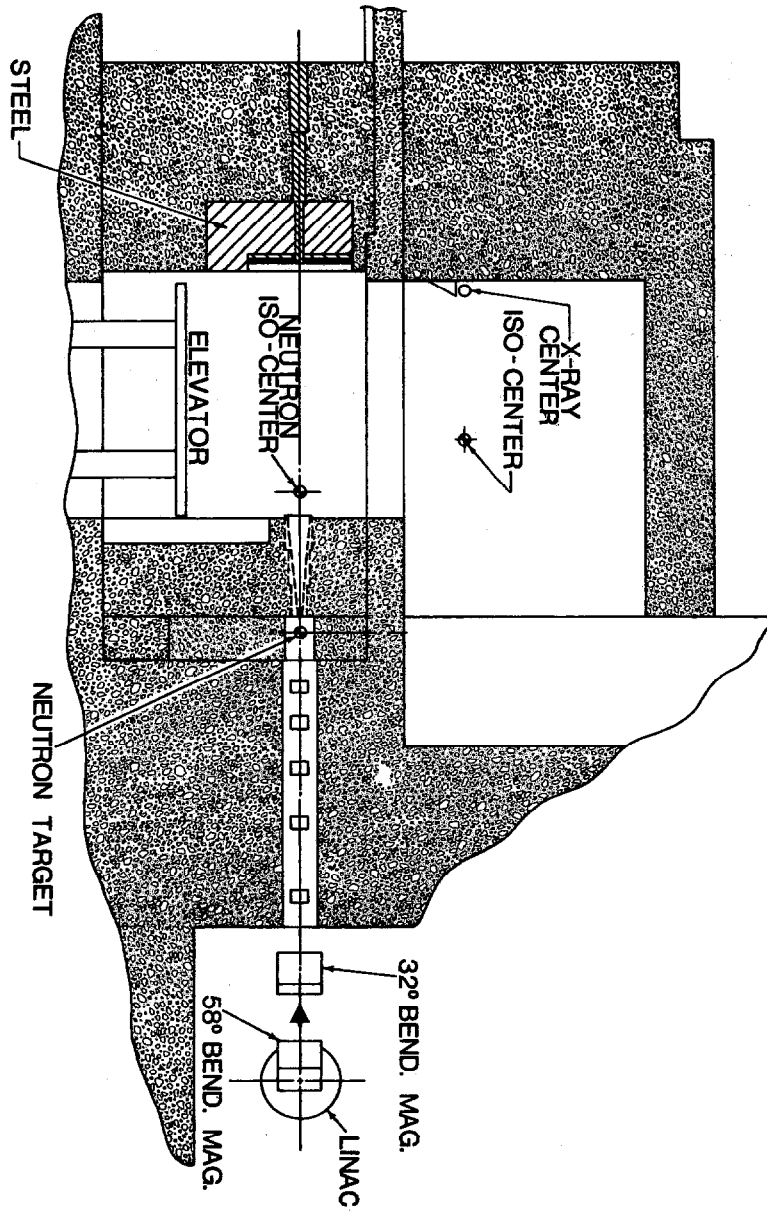
The following are the requirements that the various mechanical components of the alignment system have to meet.

1. Neutron-Level Laser Beams. (\*critical component)
  - a) N-S and E-W lasers coaxial.
  - b) N-S and E-W beams meet at a point, the I/C.
  - c) All four laser beams horizontal.
  - d) N-S and E-W beams cross at 90°.
  - \*e) E-W lasers coaxial with neutron beam.
  - f) N-S lasers beam is at 153.2 cm from center of Be-target.
2. X-ray Level Laser Beams.
  - a) Same as for n-lasers, except W-laser beam meets center line lead marker of X-ray system.
  - b) Same as for n-lasers.
  - c) Same as for n-lasers.
  - d) Same as for n-lasers.
  - \*e) E-W lasers beam coincident with lower beam when platform raised.
  - f) N-W lasers beam is at 102.1 cm from reference face of markers graticule.
  - g) Cross-lines of lasers are symmetrical around the isocenter.
3. Chair, Rails, Platform.
  - a) Rails are parallel with E-W lasers beam at n-level.
  - \*b) Axis of rotation of base is vertical and coplanar with the E-W laser beams at n-level.
  - c) Positive stop at West end of rails makes axis of rotation of base coplanar with N-S laser beams at n-level.
  - d) Raising the platform brings marks made using E-W laser beam at n-level to E-W laser beams at x-level.
  - e) Axis of rotation of chair base stays vertical at all platform levels.
  - f) A stop on the rails brings the axis of rotation of the base coplanar with N-S lasers beam at X-level.
  - g) The rails are horizontal at all levels.
4. X-ray tube and graticule.
  - a) The cross made by the lead markers of the graticule is concentric with the E-W lasers beam (X-level).



APP. 10, pg. 2

- b) The X-ray focus is on the E-W laser's beam axis.
  - c) The X-ray focus is at 153.2 cm from the N-S lasers beam axis, and therefore the lead markers project to a spacing of 1.0 cm at the X-isoplane.
5. Field lights.
- a) The center of the light field projected by the field light filament is coincident with the E-W lasers beam.
  - b) The edges of the light field projected on the skin reproduce the edges of the neutron field at that point, defined as the 50% dose level.

[illegible]

## APPENDIX 11

### Isodose Distributions. Examples.

Figure 1(a) shows the isodose distribution for a 10x10 cm<sup>2</sup> field at 153.2 cm SSD. The 100% normalization dose is that at 1.7 cm deep on the central axis.

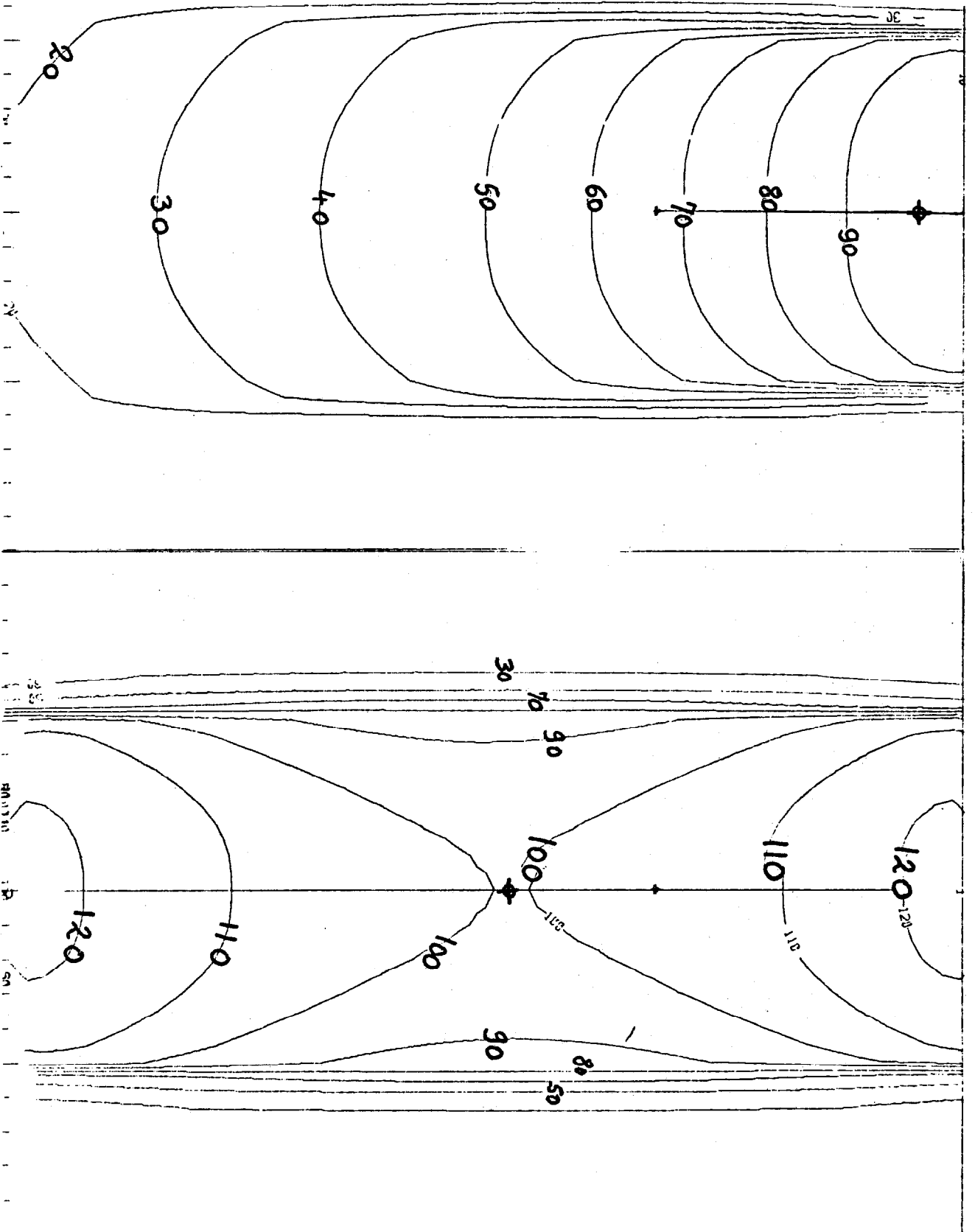
Figure 1(b) shows the effect of two parallel opposed 10x10 cm<sup>2</sup> fields, both at 153.2 cm SSD, separated by 30 cm of tissue. Normalization is at 15 cm deep, both fields contributing equal doses at that point.

Figure 2(a) shows the isodose distribution for a 10x10 cm<sup>2</sup> field as above, but with a "45°" wedge filter as described in Appendix 9. Normalization is at 1.7 cm deep on the central axis.

Figure 2(b) shows the effect of combining two wedged fields at 90° to each other, with the wedges oriented as shown. Normalization is at 10 cm deep, where the central axes cross and both fields contribute equal doses.

Figure 3 shows a typical head and neck treatment plan. Four fields are used: two parallel opposed, 10 cm wide, and two posterior obliques with wedges as shown, 6 cm wide. The two opposed fields contribute equal doses to the midplane and are prescribed for 6 treatments. The two obliques are "loaded" 2:1 in favor of the field on the left, i.e., it contributes twice the dose than the other at their intersection (also on the midplane), and are prescribed for 8 treatments. Normalization is to the sum of the doses each field contributes to the midplane. The spinal cord receives less than 50% of this normalization dose.

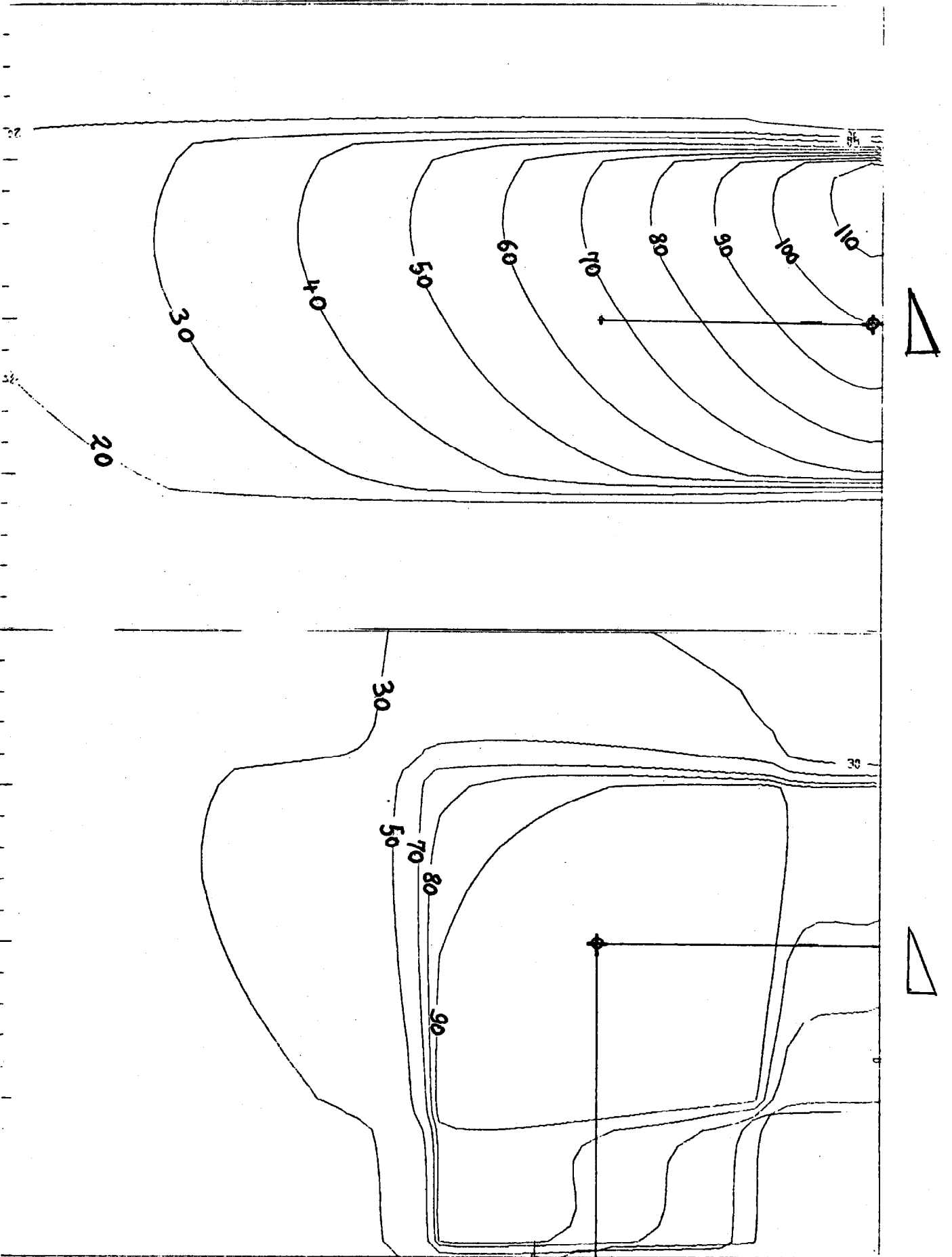
Figure 4 shows an example of mixed beam planning, in this case of an esophageal tumor. Figure 4(a) shows the neutron component, delivered through two parallel opposed fields, and contributing 800 rad to the center of the tumor. Figure 4(b) shows the photon component, delivered through two angled fields from a 4MeV linear accelerator, and contributing 4000 rad to the center of the tumor. Figure 4(c) shows the combined isodose distribution of the two components, where the neutron dose has been increased by a biological effect factor (RBE) of 3.0 to contribute 2400 rad equivalent to the center of the tumor. Normalization was done in each case to the sum of the doses at the center of the tumor. In Figure 4(c), the 93% isodose curve (also shown) encompasses the target volume for a "minimum target dose" of  $(4000 + 2400) \times .93 = 6000$  rad equivalent.



(a)

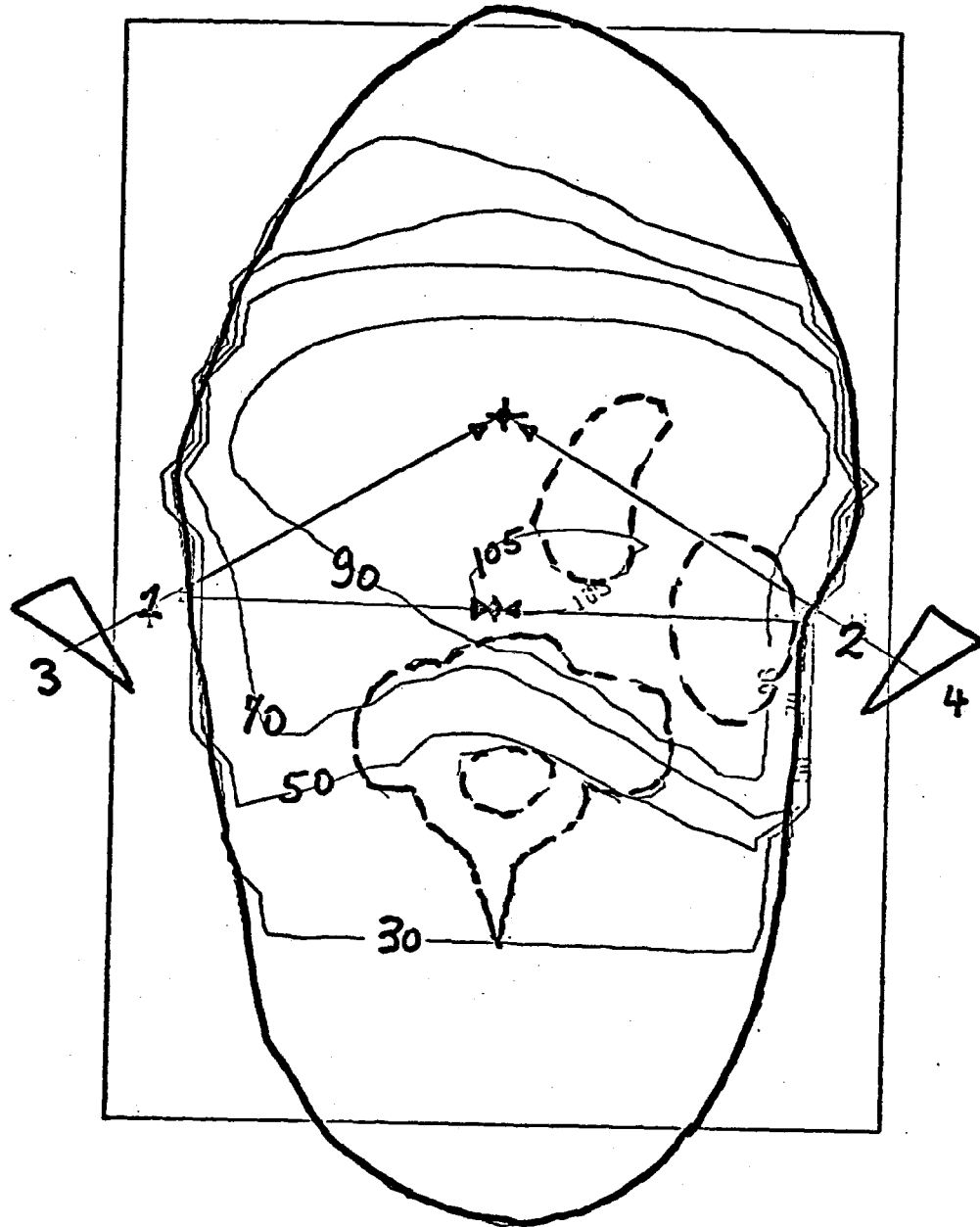
APP. 11, Fig. 1

(b)

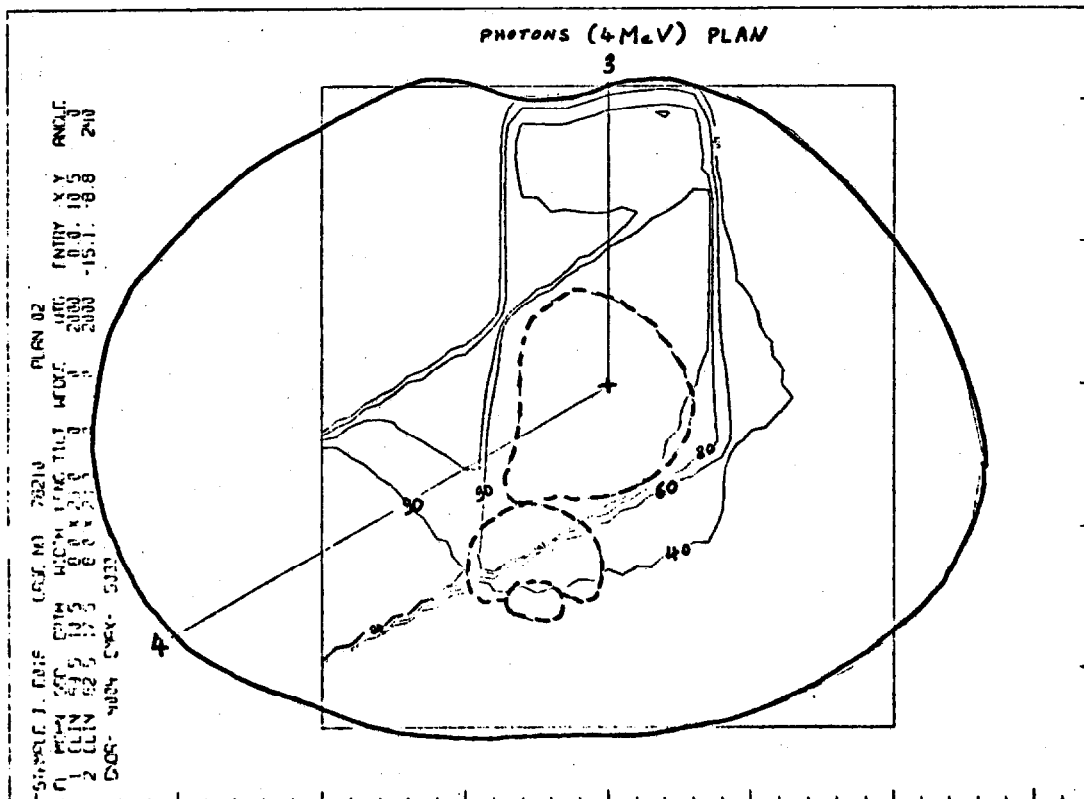
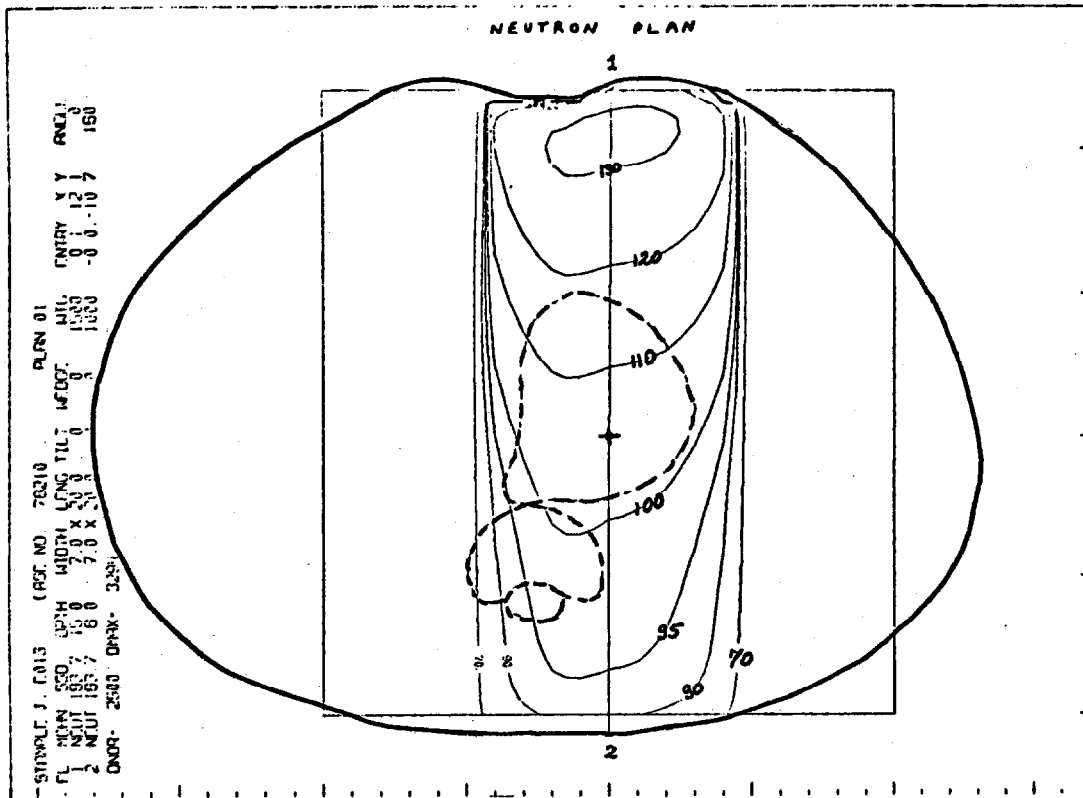


(a)

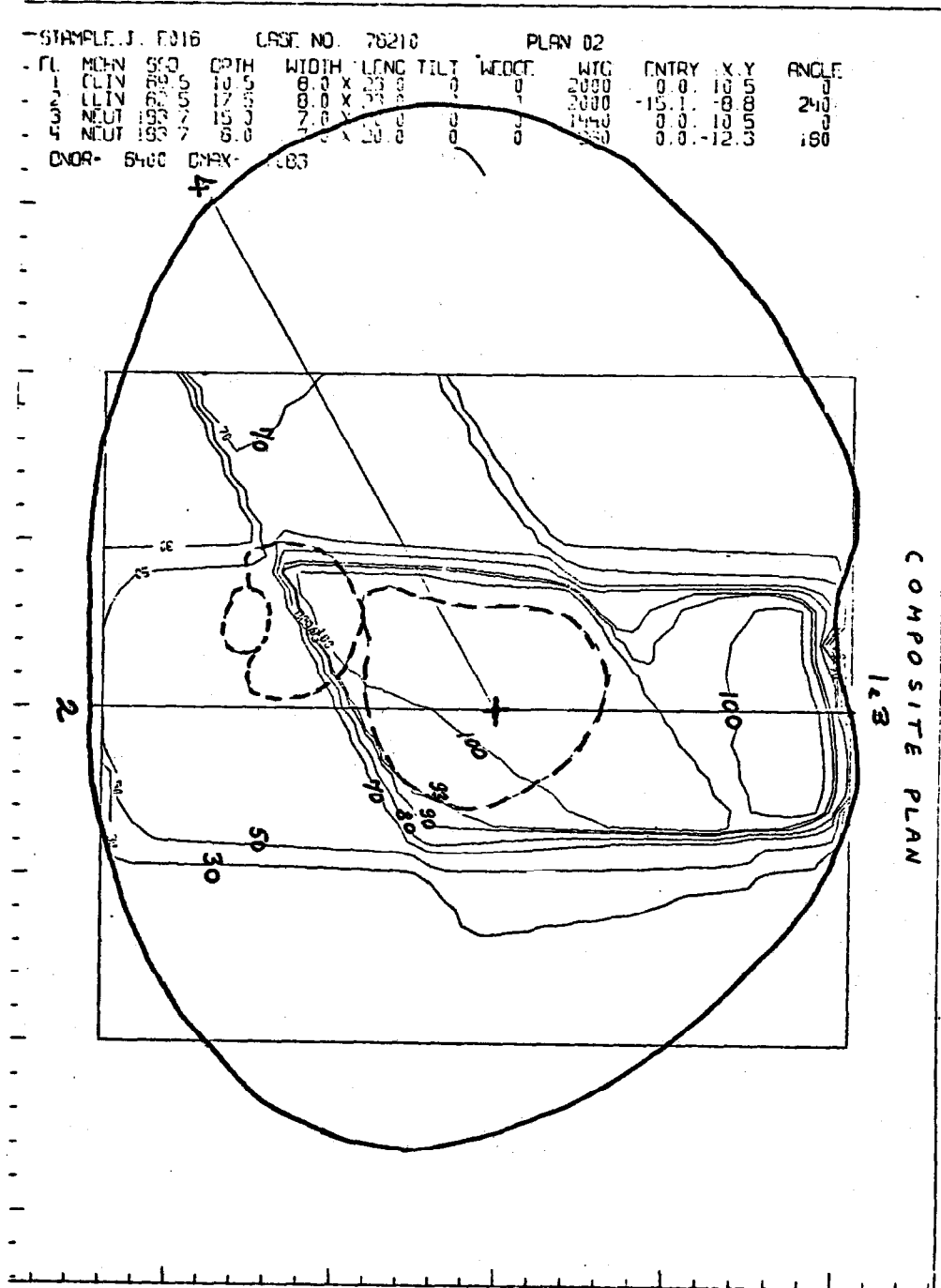
APP. 11, Fig. 2



APP. 11, Fig. 3



APP. 11, Fig. 4



APP. 11, Fig. 4(c)

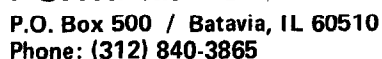


APPENDIX 12

Radiotherapy Documents.

Following is a copy of the treatment record chart developed at the Cancer Therapy Facility using as a model charts from Michael Reese Hospital and other centers. The set-up sheets for various anatomical sites, also shown, are used each treatment for easy repositioning of the patient and are always kept, together with isodose distributions, check films and medical notes, in a treatment folder.

Also shown are some diagramatic forms for various tumor sites, with room for both neutron and photon treatment descriptions. These forms are used for mixed modality treatments and are a valuable help in communication between Fermilab and the referring institutions.



DATE \_\_\_\_\_

**SURGERY:**      Yes      No

\*DOSE PRESCRIBED AT \_\_\_\_\_%\_\_\_\_\_.M.D.

$$MU = \frac{(TD/f_x \cdot f_{ld})}{\text{calculated}} \cdot X1 = 470 \cdot MU = \text{back up dosimeter}$$

NAME:

I.D. #:

SPECIAL INSTRUCTIONS:

CUMULATIVE DOSE

DAILY

SITE

X  
R  
A  
Y

N  
E  
U  
R  
O  
G  
R  
A  
M

NOTES: CHANGES IN TREATMENT;  
SKIN, MUCOSA REACTIONS;  
NODE REGRESSION, ETC.

No.	SITE		
SAD / SSD		CHAIR	ANGLE
COLLIMATOR		TILT	
WEDGE No.		ORIENTATION	
BLOCK No.		POSITION	
BLOCK No.		POSITION	
BUILD UP		SIZE	
FREQ		FRACTIONS	
MU	JIGGY	DATE	
X1	Set		
DATE		DAYS	SIGN.

								1		1	
								2			
								3			
								4			
								5			
								6			
								7			
								8			
								9			
								10			
								11			
								12			
								13			
								14			
								15			
								16			
								17			
								18			
								19			
								20			
								21			
								22			
								23			
								24			
								25			
								26			

I.D. # \_\_\_\_\_

**PAGE 4**



Name \_\_\_\_\_ I.D. # \_\_\_\_\_

[illegible]



**CONSENT TO PARTICIPATE IN RESEARCH EXPERIMENT**

I, \_\_\_\_\_ have read the booklet entitled "NEUTRON RADIATION THERAPY RESEARCH PROJECT" (Rev. 1). I have been informed that I have a cancer of a type that is under study in the research project described in the booklet. I understand that by signing this form I am consenting to participate in the experiment to determine the effectiveness of neutron radiation for my kind of cancer, \_\_\_\_\_  
(cancer site)

I understand that there are risks and side effects associated with radiation treatment. I have read the leaflet explaining possible risks and complications of radiation for my kind of cancer, and I understand them. All of my questions with regard to the experiment, the risks and side effects, have been answered.

I understand that my records will be confidential. I understand that I may receive no benefit from my treatment, no promises have been made to me. I understand that I am free to withdraw from this experiment at any time without jeopardy to my future treatment. I have read and I understand this consent form. I have had at least twenty-four hours to think whether I wish to participate and to discuss this matter with my family, friends and doctors.

I hereby agree and consent to participate in the experiment as described in the booklet entitled "NEUTRON RADIATION THERAPY RESEARCH PROJECT" (Rev. 1).

\_\_\_\_\_  
*Patient's Signature*

\_\_\_\_\_  
*Witness*

**PICTURE**

\_\_\_\_\_  
*Date*

I have explained this research treatment to this patient and/or relative(s).

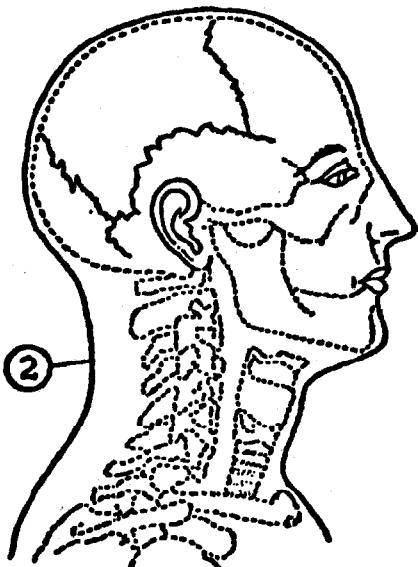
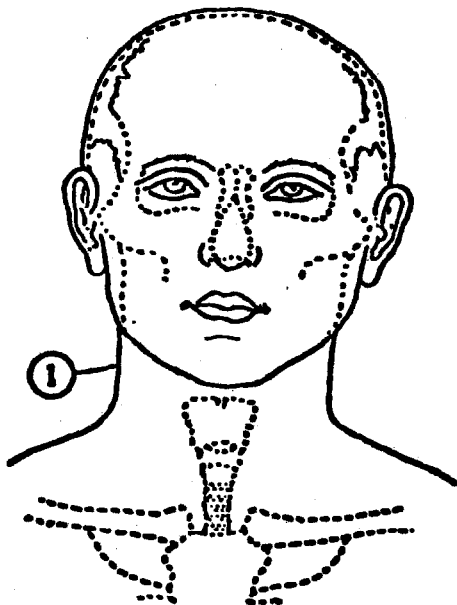
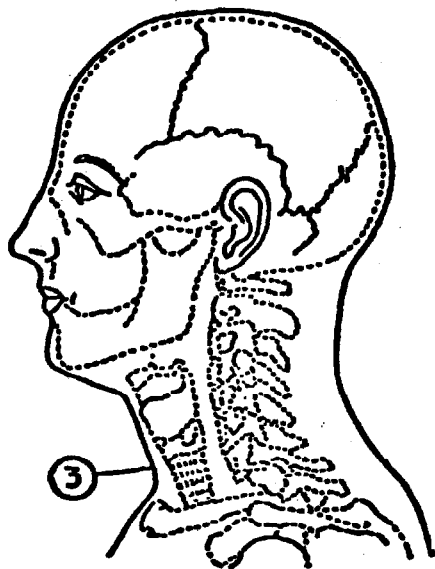
\_\_\_\_\_  
*Signature of Fermilab Radiation Therapist* M.D.





**Patient Name:** \_\_\_\_\_

Date: from 1/1  
to 1/1



	FIELD NUMBER			
SAD or SSD				
CHAIR ANGLE				
COLLIMATOR ANG.				
TONGUE BLADE				
BLOCK				
BOLUS (size )				
WEDGES (no. )				

CHAIR FIXTURES: \_\_\_\_\_

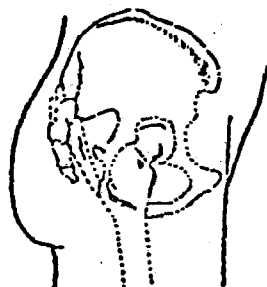
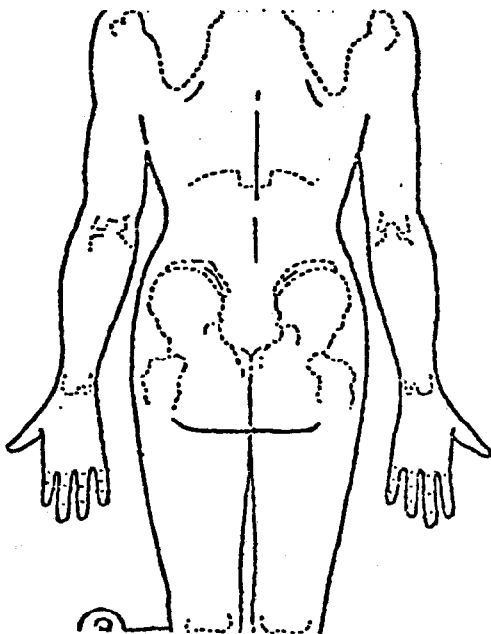
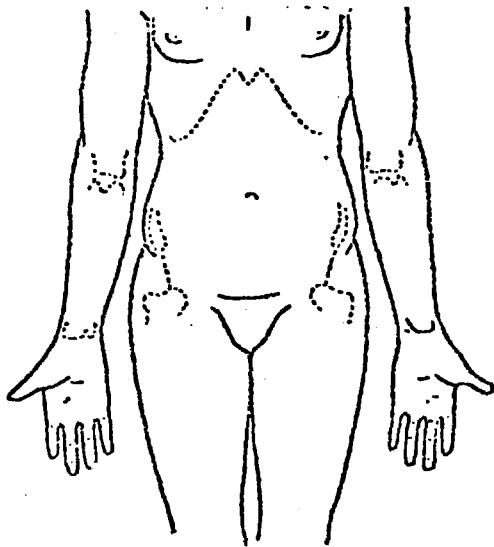
TREATMENT SEQUENCE:  
FIELD NO. \_\_\_\_\_

-82-  
PATIENT SET-UP



Patient Name: \_\_\_\_\_

Date: from   /  /    
to   /  /  



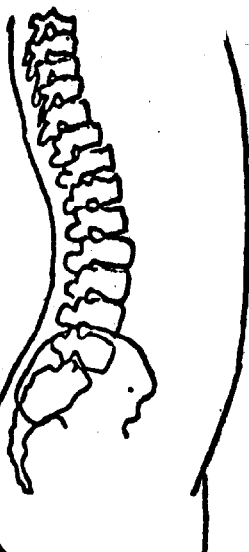
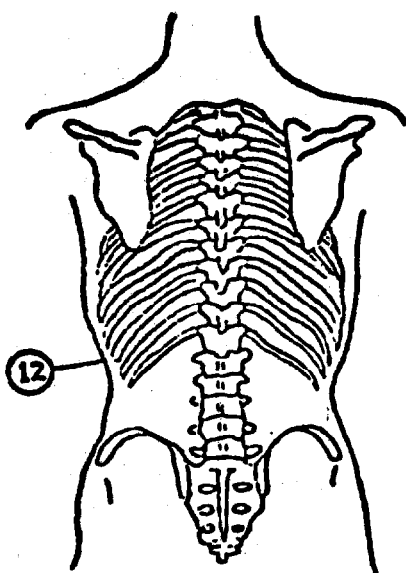
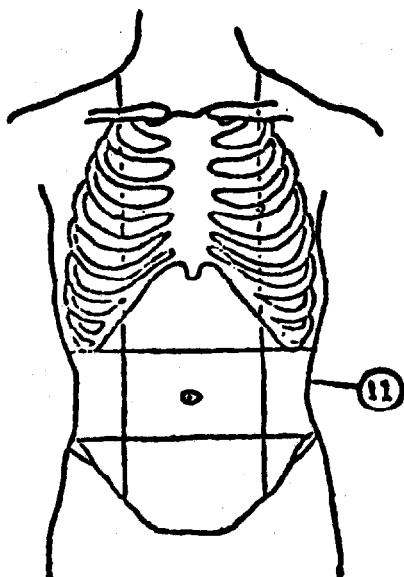
	FIELD NUMBER				
SAD or SSD					
CHAIR ANGLE					
COLLIMATOR ANG.					
TONGUE BLADE					
BLOCK					
BOLUS (size )					
WEDGES (no. )					

CHAIR FIXTURES: \_\_\_\_\_

TREATMENT SEQUENCE:

FIELD NO.

Date: from 1/1  
to 1/1



	FIELD NUMBER			
SAD or SSD				
CHAIR ANGLE				
COLLIMATOR ANG.				
TONGUE BLADE				
BLOCK				
BOLUS (size )				
WEDGES (no. )				

**CHAIR FIXTURES:**

**TREATMENT SEQUENCE:**

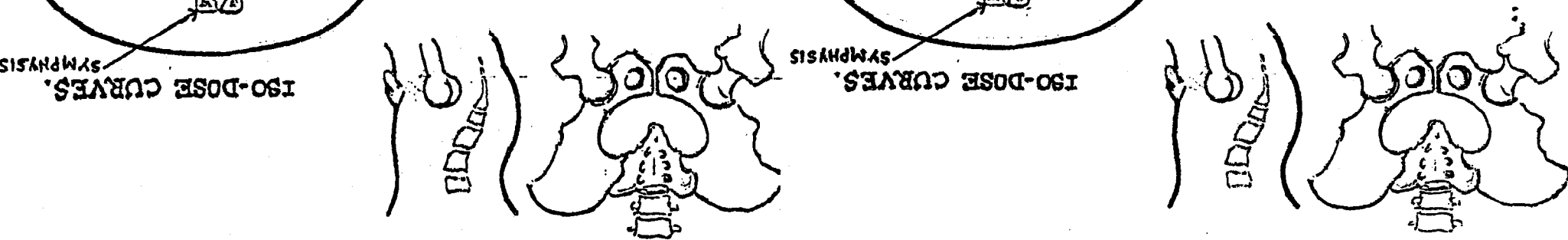
FIELD NO. / / / / /

Cancer Therapy Department

VOLUME PROPOSED	PHOTONS	NEUTRONS	Field arrangement					TOTAL RAD. EQV.	
			Dose	No. fr.	Time	fr/wk			
Pelvic fields							Min.	Max.	
Boost							Min.	Max.	
Avg. Dose to Rectum									

PHOTONS

NEUTRONS



Rectum  
 Prostate  
 SYMPHYSIS  
 ISO-DOSE CURVES.

Designed by R. Moorthy, M.D.

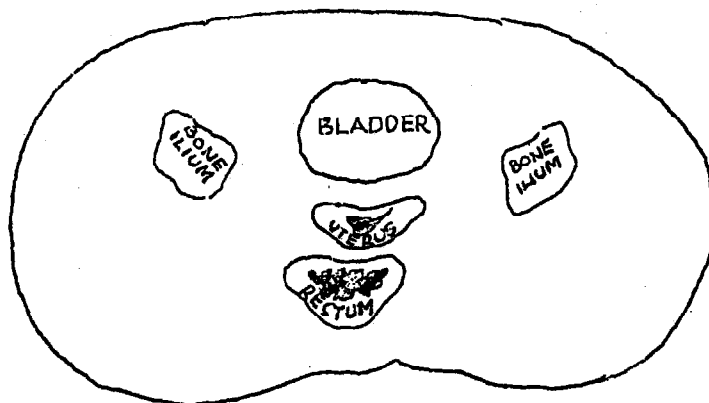
COMPOSITE CHART FOR NEUTRONS / PHOTONS / MIXED BEAM THERAPY

Fermi National Accelerator Laboratory  
P.O. Box 500 • Batavia, Illinois • 60511

INTRACAVITARY THERAPY:	
Radioactive source: Cesium---	No. of mgms. -----
Radium-----	or mg. equiv. -----
Other-----	No. of hrs -----
Dose to point A-----Point B-----	
Total mgm. hrs.-----	
(***)For any other pertinent information other side of the page can be used (***)	

PHYSICS - INFORMATION

ISODOSE CURVES FOR PHOTONS

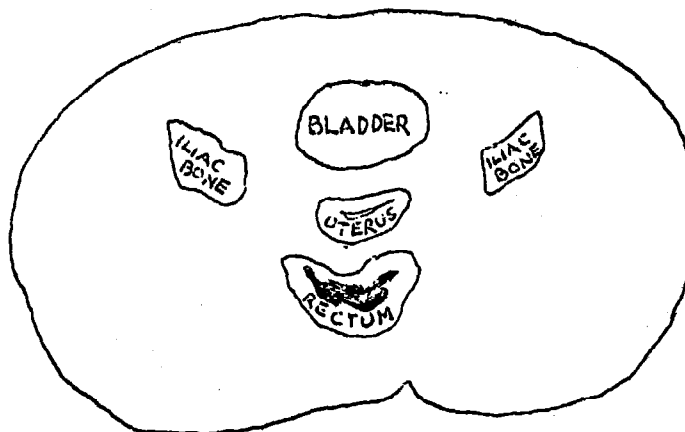


SECTION JUST ABOVE HIP JOINT

SIGNATURE-PHYSICIST

ISODOSE CURVES FOR NEUTRONS

SIGNATURE-----  
(RADIOTHERAPIST)



SECTION JUST ABOVE HIP JOINT

SIGNATURE-PHYSICIST

SIGNATURE:  
(RADIOTHERAPIST)

ANY PERTINENT ADDITIONAL INFORMATION:

**COMPOSITE CHART FOR MIXED BEAM TREATMENT FOR  
HEAD AND NECK CANCERS**

P.O. Box 500 • Batavia, Illinois • 60510

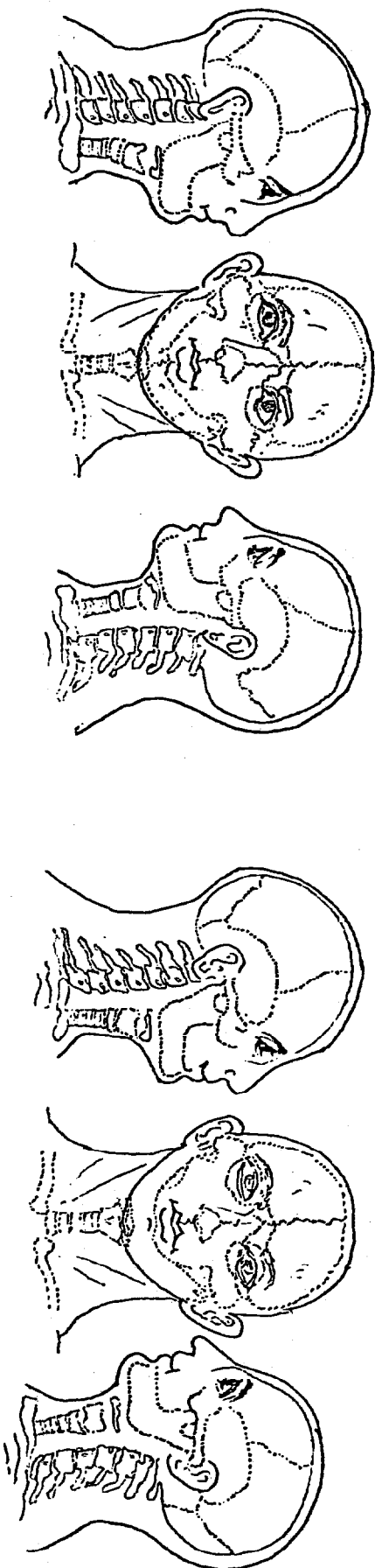
Cancer Therapy Department

NO.	Intended Target Vol.	PHOTONS					NEUTRONS					TOTAL RAD EQV.	
		Describe field Arrangement	DOSE	No. of frac.	Fr/wk.	Total Time	Describe field Arrangement	DOSE n-rads p-equiv	No. of frac.	Fr/wk	Total Time		
1.	Primary tumor Upper neck-nodes				/					/			Min..... Max.....
2.	Lower neck-nodes				/					/			Min..... Max.....
3.	Boost fields				/					/			Min..... Max.....
4.	Other.....				/					/			Min..... Max.....
SPINAL CORD DOSE		PHOTONS					NEUTRONS						

Map out the field outlines on the diagrams given below:

PHOTON BEAM TREATMENTS

NEUTRON BEAM TREATMENTS

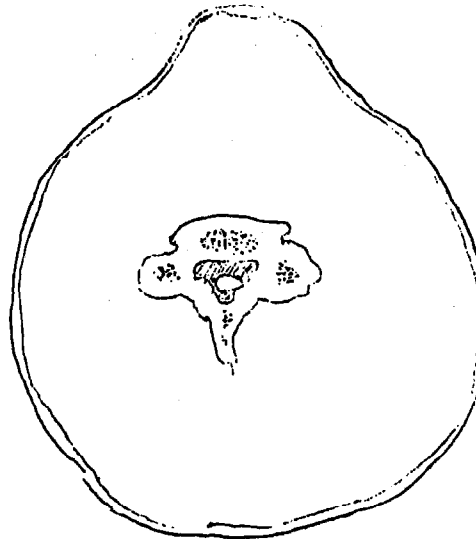


DETAILS OF PHYSICS-( PHOTON )

ISODOSE CURVES-PHOTON BEAM

RADIOTHERAPIST COMMENTS

\_\_\_\_\_  
\_\_\_\_\_  
\_\_\_\_\_  
\_\_\_\_\_  
\_\_\_\_\_  
\_\_\_\_\_  
\_\_\_\_\_  
\_\_\_\_\_  
\_\_\_\_\_  
\_\_\_\_\_  
\_\_\_\_\_  
\_\_\_\_\_



\_\_\_\_\_  
\_\_\_\_\_  
\_\_\_\_\_  
\_\_\_\_\_  
\_\_\_\_\_  
\_\_\_\_\_  
\_\_\_\_\_  
\_\_\_\_\_  
\_\_\_\_\_  
\_\_\_\_\_  
\_\_\_\_\_  
\_\_\_\_\_

Physicist's Signature \_\_\_\_\_

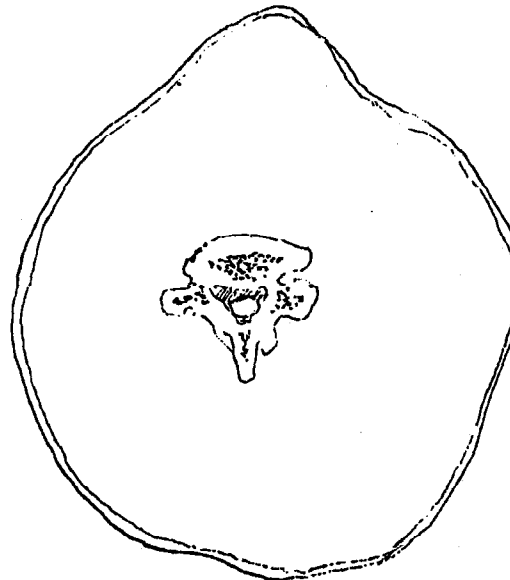
RADIOTHERAPIST'S SIGNATURE \_\_\_\_\_

DETAILS OF PHYSICIS ( NEUTRONS )

ISODOSE CURVES-NEUTRON BEAM

RADIOTHERAPIST COMMENTS  
( NEUTRONS )

\_\_\_\_\_  
\_\_\_\_\_  
\_\_\_\_\_  
\_\_\_\_\_  
\_\_\_\_\_  
\_\_\_\_\_  
\_\_\_\_\_  
\_\_\_\_\_  
\_\_\_\_\_  
\_\_\_\_\_  
\_\_\_\_\_  
\_\_\_\_\_



\_\_\_\_\_  
\_\_\_\_\_  
\_\_\_\_\_  
\_\_\_\_\_  
\_\_\_\_\_  
\_\_\_\_\_  
\_\_\_\_\_  
\_\_\_\_\_  
\_\_\_\_\_  
\_\_\_\_\_  
\_\_\_\_\_  
\_\_\_\_\_

Physicist's Signature \_\_\_\_\_

RADIOTHERAPIST'S SIGNATURE \_\_\_\_\_



# MIXED BEAM RADIATION TREATMENTS FOR CARCINOMA

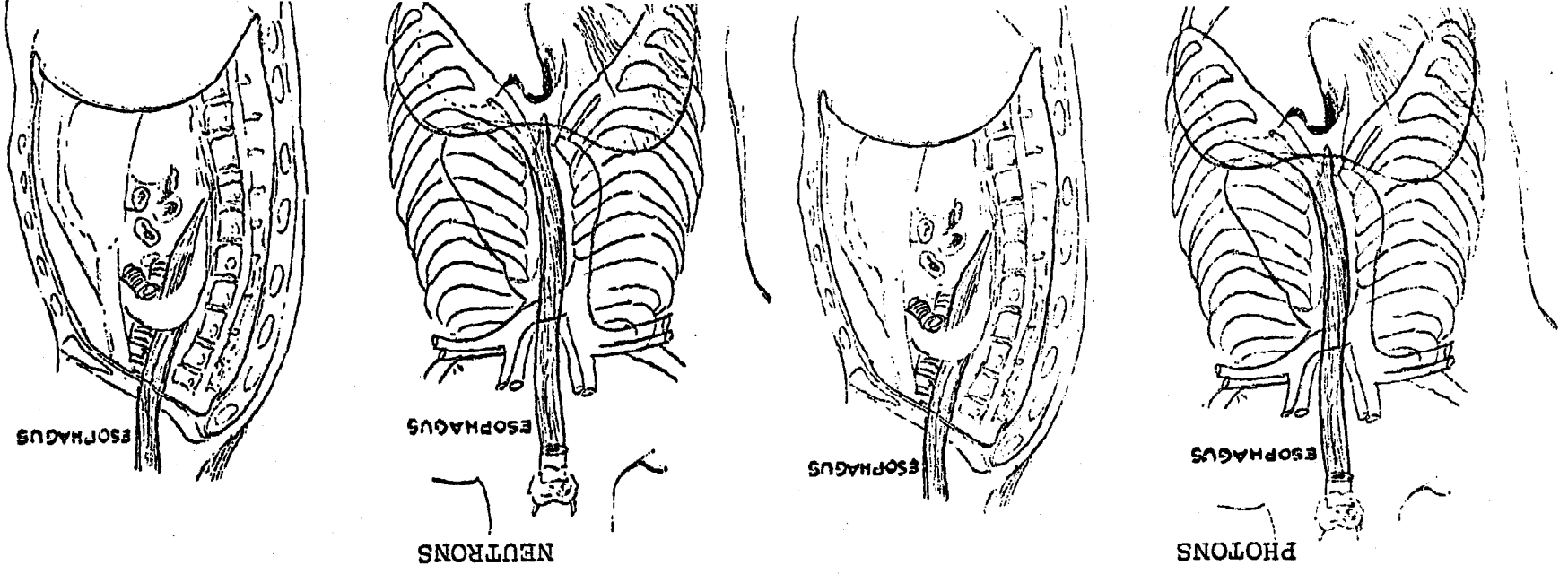
Fermil National Accelerator Laboratory  
 P.O. Box 500 • Batavia, Illinois • 60510

Cancer Therapy Department

## ESOPHAGUS

VOLUME		PHOTONS							NEUTRONS							TOTAL RAD EQ	
PROPOSED	field arrangement	Dose	No. of	Time	fr/wk.	field arrangement	Dose	n-rads	p-equiv	No. of	Time	fr/wk.	TOTAL RAD EQ				
-89-	*Cervico												Min.	TOTAL RAD EQV			
	thoracic																
	or												Max.	TOTAL RAD EQV			
	*thoracic																
	or												Min.	TOTAL RAD EQV			
	*thoraco																
	abdomen												Max.	TOTAL RAD EQV			
	and or																
	*supracl.												Min.	TOTAL RAD EQV			
	Boost to primary																

\*\*\*Please map out the radiation fields over the skeletal diagrams given below:\*\*\*



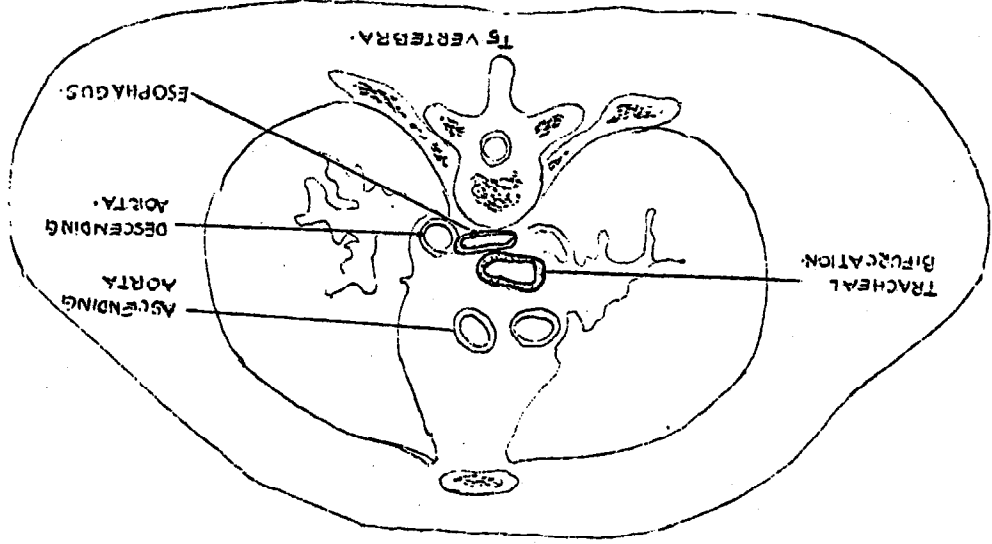
Designed by  
 R. Moorthy,  
 M.D.

PHYSICS CALCULATIONS

SIGNATURE-PHYSICIST

SIGNATURE-PHYSICIST

-90-



ISODOSE DISTRIBUTION CURVES

Neutrons

RADIO THERAPIST'S REMARKS



ISODOSE DISTRIBUTION CURVES

Photons

SIGNATURE-RADIO THERAPIST

(Print)

ADDITIONAL INFORMATION/REMARKS etc.

### APPENDIX 13

#### Evolution of the Treatment Room

This historical appendix has recollections on the evolution of a humble freight elevator into the floor of the most active fast neutron radiation therapy room in the United States, as of December, 1978.

The Fermilab Cancer Therapy Facility (CTF) was built with funds provided by Chicago foundations, private organizations, private individuals, the American Cancer Society - Illinois Division, and the Illinois Cancer Council. These funds amounted to less than \$300,000. Because funds were known to be very limited, the CTF was built indoors, as close to the linac itself as possible, and as much surplus and unwanted/obsolete materials were employed as possible. The existence of an infrequently used freight elevator and the need to adjust the height of the patient to utilize properly the fixed horizontal beam created an obvious match. This elevator is 8 ft. wide and 9 ft. long in the beam direction.

All the shielding used, but for a small part of one wall, was either existing linac shielding, surplus heavy concrete shielding from the defunct Princeton-Pennsylvania Accelerator, or was heavy concrete cast in place.

The shielding door to the treatment room was an air cushioned ordinary concrete door measuring approximately 7 ft. x 5 ft. x 7 ft. (high). This door was very effective in stopping neutrons but the noise of the air compressor needed to "float" it was unbearable to staff and patients. Hence, the CTF is now operated with the air door closed to form a 24 inch wide access tunnel and an external 12 inch boron loaded polyethylene door furnishes a barely acceptable neutron shield. During radiobiology experiments, the air door is used. Otherwise, the neutron field outside would lead to the absorption of unacceptably high occupational doses by experimenters and CTF staff.

The original rails to translate the patient supporting fixture, the fixture base capable of rotation and permitting orthogonal motions of the fixture with respect to the vertical axis of rotation, and the original patient fixtures have all been replaced during the last year. The rails and wheels combination were replaced by ball bushings and appropriate cylindrical rails. A new fixture base was built incorporating a shaft encoder to read the angle of the chair, DC motors with computer compatible power supplies, and powered X-Y adjustments. Initially two completely different fixtures were used. One had been built using an office chair and another one was built with a removable cafeteria chair. The first fixture was used mainly for head and neck as well as brain irradiations. The second

APP. 13, page 2

one was used (a) with a chair for esophagus, pancreas, and breast irradiations, and (b) in the standing up position for bladder, cervix, prostate, and leg osteosarcoma. This fixture had adjustable arm supports. The new fixture has all the features of both the previous fixtures but it may be reconfigured in one to two minutes using components fixed to a minimum base frame using toggle fasteners.

Initially, an SAD of 153.2 cm. was used with an isocenter-collimator end spacing of 28 cm. Ample knee space had been provided. In practice, we found that frequently the new fixture and the collimator holder were in physical conflict. The wall and collimator holder have therefore, been shortened by 6 inches. A new collimator system was designed, built and new shorter collimators are being cast. Parts of the new system have already been installed.

An overhead monorail lift had been installed to handle "large" collimators since they weigh up to some 200 lb. However, it has been found more practical to increase the SAD rather than use the larger heavier collimators when larger field sizes were required.

The aesthetic appearance of the treatment room has been improved by the addition of cheerful wall paper and wood paneling, the installment of a false floor (with carpeting) over the original freight elevator floor and the gradual removal of unsightly cables and non-essential equipment. Piped music has been added recently and the patients have reacted enthusiastically.

## APPENDIX 14

### Charge Integrators

Figure 1 is the circuit schematic of the charge integrators in use at the CTF. It must be remembered that the Fermilab injection accelerators work at 15Hz and that they have a very small duty cycle. Hence, the use of mechanical reed relays is possible. Critical components are listed separately. Non-critical components are called in the schematics directly.

The output amplifier with a nominal gain of ten is used both to increase sensitivity and to provide long cable drive capabilities. The output from the integrators are connected to the differential inputs of a multiplexed twelve bit analog to digital converter.

The effective integrating capacitance is given approximately by  $C_{eff} = C_f \frac{R_3}{R_4}$ .

The range of capacitances of the integrating capacitors used is 30pF to 20nF. Since  $R_4/R_3$  is approximately 10 in our integrators,  $C_{eff}$  ranges from 3pF to 2nF.

The selection of the reed relay is critical. Some reeds are noisy and others are very quiet. At the CTF, they are selected by trial in the individual integrator in which they will be used. A reed relay suitable for a  $C_{eff} = 500pF$ , may not be suitable for an integrator with  $C_{eff} = 3pF$ .

---

#### List of Critical Components

---

- A1 - Keithley #302 operational amplifier selected to meet manufacturer's specs.
  - A2 - Analog Devices 40K operational amplifier.
  - R1 - 100M $\Omega$  - metal film.
  - R2 - 10M $\Omega$  for  $C_f = 50pf$ ; 27K $\Omega$  for  $C_f = 20nf$ .
  - R3 - 10K $\Omega$   $\pm$  1% - metal film.
  - R4 - 100K $\Omega$   $\pm$  1% - metal film.
  - P1 - 20K $\Omega$  - 10 turn potentiometer.
  - P2 - 100 $\Omega$  - 10 turn potentiometer.
  - C1 - 200pF polystyrene capacitor.
  - C2 - 0.001  $\mu F$ .
  - C3 - 0.001  $\mu F$ , 1KV.
  - Cf - hermetically sealed polystyrene capacitor.
  - RR - Hamlin MRH-15-185.
  - D1 - 1N4002.
  - COIL - JAMES 7805.
  - +15, -15V PS - Analog Device 902.
-

APP. 14, Fig. 1

